

AD-A061 140

ARMY ENGINEER WATERWAYS EXPERIMENT STATION VICKSBURG MISS F/G 18/3
RESPONSE OF LINEAR ELASTIC TRANSVERSE-ISOTROPIC MEDIA TO BOREHO--ETC(U)
SEP 78 G Y BALADI , M E GEORGE
WES-TR-S-78-12

UNCLASSIFIED

NL

1 OF
AD A061140



DDC FILE COPY

AD A061140



LEVEL II

2



TECHNICAL REPORT S-78-12

RESPONSE OF LINEAR ELASTIC TRANSVERSE-ISOTROPIC MEDIA TO BOREHOLE PRESSUREMETER LOADINGS.

by

10 George Y. Baladi and Michael E. George

Geotechnical Laboratory

U. S. Army Engineer Waterways Experiment Station
P. O. Box 631, Vicksburg, Miss. 39180

12 57p.

11 September 1978

9 Final Report, 1974-1975

Approved For Public Release; Distribution Unlimited

14 WES-TR-S-78-12

DDC
NOV 13 1978Prepared for Director, Defense Nuclear Agency
Washington, D. C. 20305Under DNA Subtask SB209, Work Unit 40, "Material Model
Development and Ground Shock Calculations"

78 11 08 046

038 100

JOB

Destroy this report when no longer needed. Do not return
it to the originator.

Unclassified

SECURITY CLASSIFICATION OF THIS PAGE (When Data Entered)

REPORT DOCUMENTATION PAGE		READ INSTRUCTIONS BEFORE COMPLETING FORM
1. REPORT NUMBER Technical Report S-78-12 ✓	2. GOVT ACCESSION NO.	3. RECIPIENT'S CATALOG NUMBER
4. TITLE (and Subtitle) RESPONSE OF LINEAR ELASTIC TRANSVERSE-ISOTROPIC MEDIA TO BOREHOLE PRESSUREMETER LOADINGS		5. TYPE OF REPORT & PERIOD COVERED Final report
		6. PERFORMING ORG. REPORT NUMBER
7. AUTHOR(s) George Y. Baladi Michael E. George		8. CONTRACT OR GRANT NUMBER(s)
9. PERFORMING ORGANIZATION NAME AND ADDRESS U. S. Army Engineer Waterways Experiment Station Geotechnical Laboratory P. O. Box 631, Vicksburg, Miss. 39180		10. PROGRAM ELEMENT, PROJECT, TASK AREA & WORK UNIT NUMBERS See Block 18
11. CONTROLLING OFFICE NAME AND ADDRESS Defense Nuclear Agency Washington, D. C. 20305		12. REPORT DATE September 1978
		13. NUMBER OF PAGES 53
14. MONITORING AGENCY NAME & ADDRESS (if different from Controlling Office)		15. SECURITY CLASS. (of this report) Unclassified
		15a. DECLASSIFICATION/DOWNGRADING SCHEDULE
16. DISTRIBUTION STATEMENT (of this Report) Approved for public release; distribution unlimited.		
17. DISTRIBUTION STATEMENT (of the abstract entered in Block 20, if different from Report)		
18. SUPPLEMENTARY NOTES This work was sponsored by the Defense Nuclear Agency under Nuclear Weapons Effects Subtask SB209, Work Unit 40, "Material Model Development and Ground Shock Calculations."		
19. KEY WORDS (Continue on reverse side if necessary and identify by block number) BOREHOLE (Computer program) Isotropic materials Boreholes Pressure gages Boundary value problem Pressure measurement Elastic materials Transverse-isotropic materials		
20. ABSTRACT (Continue on reverse side if necessary and identify by block number) This report documents the development of a closed form solution to the idealized borehole pressuremeter problem in linear elastic transverse isotropic media. The borehole was assumed to be infinitely long and pressurized by a static pressure. The mathematical equations for the distribution of stresses and displacements anywhere around the borehole are derived and incorporated into the computer program BOREHOLE. (Continued)		

DD FORM 1 JAN 73 1473

EDITION OF 1 NOV 65 IS OBSOLETE

Unclassified

SECURITY CLASSIFICATION OF THIS PAGE (When Data Entered)


78 11 08 046

Unclassified

SECURITY CLASSIFICATION OF THIS PAGE(When Data Entered)

20. ABSTRACT (Continued).

Cont → The solution is relevant to the field determination of constitutive properties for use in ground shock calculations. It shows that, in theory, the pressure versus borehole volume change relations from a series of borehole pressuremeter tests inclined at different angles can be used to deduce an appropriate set of linear elastic transverse-isotropic constitutive properties for a given medium and provide an index to the degree of anisotropy of the material.



Unclassified

SECURITY CLASSIFICATION OF THIS PAGE(When Data Entered)

PREFACE

This study was conducted by the U. S. Army Engineer Waterways Experiment Station (WES) for the Defense Nuclear Agency under Nuclear Weapons Effects Subtask SB209, Work Unit 40, "Material Model Development and Ground Shock Calculation."

The investigation was conducted and the report prepared by Dr. G. Y. Baladi and Mr. M. E. George during the calendar years 1974-1975 under the general direction of Mr. J. P. Sale, Chief, Geotechnical Laboratory, and Dr. J. G. Jackson, Jr., Chief, Soil Dynamics Division.

Directors of WES during the preparation and publication of this report were COL G. H. Hilt, CE, and COL J. L. Cannon, CE. Mr. F. R. Brown was Technical Director.

ACCESSION for	
NTIS	White Section <input checked="" type="checkbox"/>
DDC	Buff Section <input type="checkbox"/>
UNANNOUNCED	<input type="checkbox"/>
JUSTIFICATION	
BY	
DISTRIBUTION/AVAILABILITY CODES	
Doc	SPECIAL
A	

CONVERSION FACTORS, U. S. CUSTOMARY TO METRIC (SI)
UNITS OF MEASUREMENT

U. S. customary units of measurement used in this report can be converted to metric (SI) units as follows:

<u>Multiply</u>	<u>By</u>	<u>To Obtain</u>
degrees (angle)	0.01745329	radians
inches	2.54	centimetres
kips (force)	4448.222	newtons
pounds (mass) per cubic foot	16.01846	kilograms per cubic metre

CONTENTS

	<u>Page</u>
PREFACE-----	1
CONVERSION FACTORS, U. S. CUSTOMARY TO METRIC (SI) UNITS OF MEASUREMENT-----	2
CHAPTER 1 INTRODUCTION-----	5
1.1 Background-----	5
1.2 Objective-----	7
1.3 Scope-----	7
CHAPTER 2 PROBLEM GEOMETRY, BOUNDARY CONDITIONS, AND CONSTITUTIVE AND FIELD EQUATIONS-----	8
2.1 General-----	8
2.2 Problem Geometry-----	8
2.3 Constitutive Equations-----	9
2.4 Transformation of the Elastic Properties-----	10
2.5 Field Equations-----	12
2.6 Representation of the Boundary Condition-----	14
2.7 Stresses and Displacements in Cylindrical Coordinate Systems-----	14
CHAPTER 3 DERIVATION OF THE GENERAL SOLUTION OF THE PROBLEM-----	21
3.1 General-----	21
3.2 Stress Function-----	22
3.3 Complex Representation of Stresses and Displacements-----	27
3.4 Determination of the Stress Function-----	30
3.5 Spatial Stress Distribution for Sample Problem-----	34
3.6 Spatial Displacement Distribution for Sample Problem-----	35
CHAPTER 4 CONCLUSIONS AND RECOMMENDATIONS-----	44
REFERENCES-----	45
APPENDIX A: NOTATION-----	47

LIST OF ILLUSTRATIONS

<u>Figure</u>		<u>Page</u>
2.1	Problem geometry-----	19
2.2	Two-dimensional element from the boundary-----	20
3.1	Distribution of radial and tangential stresses along the radius for $\theta = 0$ degrees at an angle of inclination of 30 degrees-----	36
3.2	Contour for radial stress at an angle of inclination of 30 degrees-----	37
3.3	Distribution of tangential stress along the boundary of the borehole whose angle of inclination is 30 degrees----	38
3.4	Distribution of radial and shear stresses along the boundary of the borehole whose angle of inclination is 30 degrees-----	39
3.5	Distribution of radial displacement u_r along the radius for $\theta = 0$ and 90 degrees at an angle of inclination of 30 degrees-----	40
3.6	Contour for radial displacement at an angle of inclination of 30 degrees-----	41
3.7	Distribution of radial and tangential displacements along the boundary of the borehole whose angle of inclination is 30 degrees-----	42
3.8	Contour for tangential displacement at an angle of inclination of 30 degrees-----	43

LIST OF TABLES

<u>Table</u>		<u>Page</u>
2.1	Direction cosines-----	16
2.2	Values of q_{ij} in the formulas of transformations (Equation 2.3)-----	16
2.3	Value of C_{ij}^I from Equation 2.1-----	17
2.4	Value of C_{ij} from Equation 2.3-----	18

RESPONSE OF LINEAR ELASTIC TRANSVERSE-ISOTROPIC MEDIA
TO BOREHOLE PRESSUREMETER LOADINGS

CHAPTER 1

INTRODUCTION

1.1 BACKGROUND

To predict the ground shock from surface or aboveground nuclear detonation, research on the use of two-dimensional finite difference wave propagation codes that treat nonlinear hysteretic media is being conducted. To use these codes, the constitutive properties (stress-strain and strength) of the in situ earth media must be determined for fast loading rates in the unconsolidated-undrained state. Conventionally, this is done by obtaining undisturbed samples from the site and testing them in the laboratory. Inevitably, the in situ properties are altered to some extent by the sampling process. Hence, using in situ field tests that give some indication of the in situ constitutive properties is desirable.

The borehole pressuremeter (References 1-3), which measures the increase in volume per unit length,¹ ΔV , of a borehole under an increasing uniform internal pressure, P_0 , is one of several tests that can be used to infer information about the in situ constitutive properties.² This device has been used in the constitutive property investigation for several high-explosives (HE) tests (References 4-7) used as test cases to study the accuracy of and the necessary improvements in the ground shock prediction procedure.

In homogeneous isotropic linear elastic materials, the shear modulus G can be directly determined from the borehole pressuremeter test:

¹ Symbols used in this report are listed and defined in the Notation (Appendix A).

² As with any test, it has its own sources of error, the most prominent of these being volume measurement errors leading to alteration of the constitutive properties due to the drilling of the borehole.

$$G = \frac{V_0 P_0}{\Delta V} \quad (1.1)$$

where V_0 is the initial volume of a unit length of the borehole. However, real earth materials are often highly anisotropic. The interpretation of data from laboratory and/or field tests based on a mathematical constitutive relation that does not account for anisotropy may lead to erroneous conclusions.

The most common departure from a state of isotropy in an earth material is layering or stratification during its deposition. This is the case whether induced by natural causes, such as sedimentary deposits, or in the construction of fills where the earth materials are placed and compacted in horizontal lifts. For these conditions, although marked differences may be noted between the vertical and the horizontal directions, generally no direction preference will exist in the horizontal planes. Such a material is said to be transversely isotropic (References 8 and 9).

For the linear elastic transverse-isotropic material, five material constants are needed to completely describe material behavior (References 8 and 9). A technique for the determination of some or all of these five material constants in the field is of great importance to the material properties investigator. Such a technique (Reference 10) would give an early deduction of those sites that are strongly anisotropic and provide data for use in the fitting of a transverse-isotropic model (Reference 7) for the materials. It appears that a series of pressuremeter tests in boreholes inclined at several different angles to the axis of symmetry of the material will yield this information. Hence, there was a need to obtain an analytical solution for the inclined borehole pressuremeter problem. Only the special case of this problem for a transverse-isotropic material in which the axis of the test (i.e., the axis of a pressurized cylindrical cavity of infinite extent) is perpendicular to the plane of isotropy has been solved analytically (Reference 9).

1.2 OBJECTIVE

The objective of this investigation is to develop a general closed form solution to the borehole pressuremeter problem where the axis of the borehole is inclined to the plane of isotropy of an elastic transverse-isotropic medium. Such a solution can be used to determine stresses and displacements in the medium in terms of the transverse-isotropic properties of the material. It is possible, therefore, to deduce the transverse-isotropic properties of the materials in terms of the volume change of the borehole.

1.3 SCOPE

The problem geometry, boundary conditions, and constitutive and field equations are presented in Chapter 2. Chapter 3 contains the derivation of the general solution of the problem and a sample problem. Conclusions and recommendations are given in Chapter 4.

CHAPTER 2

PROBLEM GEOMETRY, BOUNDARY CONDITIONS, AND CONSTITUTIVE AND FIELD EQUATIONS

2.1 GENERAL

Because the properties of the material are directionally dependent, it is more convenient to obtain the solution of the problem in a Cartesian coordinate system first and then through a coordinate transformation to determine the stresses and the displacements in a cylindrical coordinate system. Therefore, three coordinate systems are needed. The first is a Cartesian coordinate $x'y'z'$ in which $x'y'$ is parallel to the plane of isotropy (Figure 2.1) and for which the constitutive equations for a linear elastic transverse-isotropic material are well known (References 8 and 9). The second coordinate system is also Cartesian, xyz , in which the solution of the borehole pressure-meter problem is obtained (Figure 2.1). Finally, because the problem is axisymmetric, it is convenient to transform the final results from the xyz coordinate system to a cylindrical coordinate system, $r\theta z$ (Figure 2.1b).

2.2 PROBLEM GEOMETRY

The geometry of the problem is shown schematically in Figure 2.1. Figure 2.1a shows a three-dimensional view of the problem with the relative position of the Cartesian coordinate systems $x'y'z'$ and xyz . Figure 2.1b shows a two-dimensional detailed view of the problem relative to both the cylindrical coordinates $r\theta z$ and the Cartesian coordinates xyz . The axis of symmetry of the material and the axis of symmetry of the cylindrical cavity are assumed to intersect at an angle, ψ (Figure 2.1a). Therefore, the intersection of the cylindrical cavity with the plane of isotropy forms an ellipse $A'BC'D$ in the $x'y'$ plane (Figures 2.1a and 2.1b). The intersection of the cylindrical cavity with the $r\theta$ - or xy -plane is, of course, a circle $ABCD$ (Figure 2.1a). Furthermore, it is assumed that the radius of the cylindrical cavity is b and

that its surface is under normal stress, P_0 , which does not vary along the cavity.

2.3 CONSTITUTIVE EQUATIONS

Let the $x'y'$ plane of an $x'y'z'$ coordinate system (Figure 2.1a) be the plane of isotropy of the material. The constitutive equations for a linear elastic transverse-isotropic material (References 8 and 9) are:

$$\left. \begin{aligned} \epsilon_{x'} &= \frac{1}{E} \sigma_{x'} - \frac{\nu}{E} \sigma_{y'} - \frac{\nu'}{E'} \sigma_{z'} \\ \epsilon_{y'} &= -\frac{\nu}{E} \sigma_{x'} + \frac{1}{E} \sigma_{y'} - \frac{\nu'}{E'} \sigma_{z'} \\ \epsilon_{z'} &= -\frac{\nu'}{E'} (\sigma_{x'} + \sigma_{y'}) + \frac{1}{E'} \sigma_{z'} \\ \epsilon_{x'z'} &= \frac{\sigma_{x'z'}}{2G'} \\ \epsilon_{y'z'} &= \frac{\sigma_{y'z'}}{2G'} \\ \epsilon_{x'y'} &= \frac{\sigma_{x'y'}}{2G} \end{aligned} \right\} \quad (2.1)$$

where

$\sigma_{x'}, \sigma_{y'}, \sigma_{z'}$ = total normal stress components parallel to x' -, y' -, and z' -axes, respectively

$\sigma_{x'z'}, \sigma_{y'z'}, \sigma_{x'y'}$ = total shearing stress components in $x'z'$ -, $y'z'$ -, and $x'y'$ -planes, respectively

$\epsilon_{x'}, \epsilon_{y'}, \epsilon_{z'}$ = total normal strain components parallel to x' -, y' -, and z' -axes, respectively

$\epsilon_{x'z'}, \epsilon_{y'z'}, \epsilon_{x'y'}$ = total shearing strain components in $x'z'$ -, $y'z'$ -, and $x'y'$ -planes, respectively

E = Young's modulus in the plane of isotropy

E' = Young's modulus in a plane normal to the plane of isotropy

- ν = Poisson's ratio that characterizes the transverse reduction in the plane of isotropy due to stress in the same plane
- ν' = Poisson's ratio that characterizes the transverse reduction in the plane of isotropy due to stress normal to it
- G' = shear modulus for a plane normal to the plane of isotropy
- $G = \frac{E}{2(1 + \nu)}$ = shear modulus for the plane of isotropy

The elastic properties that appear in Equations 2.1 depend on the direction of the axes of the chosen coordinate system. If the direction of the axes varies, then the elastic properties vary. Only in the case of an isotropic body the elastic properties are invariant in any orthogonal coordinate system. However, there are always unique relationships of the elastic properties in one coordinate system to the elastic properties in another coordinate system. These relationships could be derived through transformation formulas that transform one coordinate system into another. Therefore, the elastic properties that appear in Equations 2.1 for the coordinate system $x'y'z'$ could be transformed into the elastic properties for the coordinate system xyz (Figure 2.1) through transformation formulas.

2.4 TRANSFORMATION OF THE ELASTIC PROPERTIES

Let C_{ij} be the elastic properties for the coordinate system xyz and let C'_{ij} be the elastic properties for the coordinate system $x'y'z'$ (Figure 2.1a). The position of the coordinate system xyz with respect to the coordinate system $x'y'z'$ is defined by Table 2.1 and the following relations:

$$\begin{aligned}x &= x' \\y &= y' \cos \psi + z' \sin \psi \\z &= -y' \sin \psi + z' \cos \psi\end{aligned}\tag{2.2}$$

The transformation formulas that relate C_{ij} to C'_{ij} are given in Reference 9 and can be written as¹

$$C_{ij} = C'_{mn} q_{mi} q_{nj} \quad (2.3)$$

The values of q_{ij} are defined in Table 2.2 where the first index, i , indicates the number of the row and the second index, j , shows the number of the column. Thus, q_{ij} denotes the element belonging to the i^{th} row and j^{th} column; for example, $q_{11} = \delta_1^2$, $q_{43} = \eta_3 \theta_3$, $q_{56} = \theta_1 \delta_2 + \theta_2 \delta_1$, and so forth. The values of δ_n , η_n and θ_n ($n = 1, 2, 3$) are given in Table 2.1; the values of C'_{ij} can be obtained from Equations 2.1 and are given in Table 2.3; and the values of C_{ij} obtained from Equation 2.3 are given in Table 2.4.

Having determined the value of the elastic properties C_{ij} , the general constitutive equation for a linear elastic transverse-isotropic material in an xyz coordinate system may be written as:

$$\left. \begin{aligned} \epsilon_x &= \frac{1}{E} \sigma_x - \left(\frac{\nu'}{E'} \sin^2 \psi + \frac{\nu}{E} \cos^2 \psi \right) \sigma_y \\ &\quad - \left(\frac{\nu'}{E'} \cos^2 \psi + \frac{\nu}{E} \sin^2 \psi \right) \sigma_z + \left(\frac{\nu'}{E'} - \frac{\nu}{E} \right) \sin 2\psi \sigma_{yz} \\ \epsilon_y &= - \left(\frac{\nu'}{E'} \sin^2 \psi + \frac{\nu}{E} \cos^2 \psi \right) \sigma_x + \left[\frac{1}{E} \cos^4 \psi + \frac{1}{E'} \sin^4 \psi \right. \\ &\quad \left. + \left(\frac{1}{G'} - \frac{2\nu'}{E'} \right) \cos^2 \psi \sin^2 \psi \right] \sigma_y + \left[- \frac{\nu'}{E'} (\sin^4 \psi + \cos^4 \psi) \right. \\ &\quad \left. + \left(\frac{1}{E} + \frac{1}{E'} - \frac{1}{G'} \right) \cos^2 \psi \sin^2 \psi \right] \sigma_z + \left[\left(\frac{1}{E} + \frac{\nu'}{E'} \right) \cos^2 \psi \right. \\ &\quad \left. - \left(\frac{1}{E'} + \frac{\nu'}{E'} \right) \sin^2 \psi - \frac{1}{2G'} \cos 2\psi \right] \sin 2\psi \sigma_{yz} \end{aligned} \right\} \quad (2.4)$$

NOTE: Equations 2.4 are continued on following page

¹ Indices assume values 1,2...6. A repeated index is to be summed over its range. Quantities are referred to rectangular Cartesian coordinates x_i .

$$\begin{aligned}
\varepsilon_z &= - \left(\frac{\nu'}{E'} \cos^2 \psi + \frac{\nu}{E} \sin^2 \psi \right) \sigma_x + \left[- \frac{\nu'}{E'} (\sin^4 \psi + \cos^4 \psi) \right. \\
&\quad + \left(\frac{1}{E} + \frac{1}{E'} - \frac{1}{G'} \right) \cos^2 \psi \sin^2 \psi \left. \right] \sigma_y + \left[\frac{1}{E} \sin^4 \psi + \frac{1}{E'} \cos^4 \psi \right. \\
&\quad + \left(\frac{1}{G'} - \frac{2\nu'}{E'} \right) \cos^2 \psi \sin^2 \psi \left. \right] \sigma_z + \left[\left(\frac{1}{E} + \frac{\nu'}{E'} \right) \sin^2 \psi \right. \\
&\quad \left. - \left(\frac{1}{E'} + \frac{\nu'}{E'} \right) \cos^2 \psi + \frac{1}{2G'} \cos 2\psi \right] \sin 2\psi \sigma_{yz} \\
\varepsilon_{yz} &= \frac{1}{2} \left(\frac{\nu'}{E'} - \frac{\nu}{E} \right) \sin 2\psi \sigma_x + \frac{1}{2} \left[\left(\frac{1}{E} + \frac{\nu'}{E'} \right) \cos^2 \psi \right. \\
&\quad \left. - \left(\frac{1}{E'} + \frac{\nu'}{E'} \right) \sin^2 \psi - \frac{1}{2G'} \cos 2\psi \right] \sin 2\psi \sigma_y \\
&\quad + \frac{1}{2} \left[\left(\frac{1}{E} + \frac{\nu'}{E'} \right) \sin^2 \psi - \left(\frac{1}{E'} + \frac{\nu'}{E'} \right) \cos^2 \psi \right. \\
&\quad \left. + \frac{1}{2G'} \cos 2\psi \right] \sin 2\psi \sigma_z + \frac{1}{2G'} \sigma_{yz} \\
\varepsilon_{xz} &= \frac{1}{2G'} \cos^2 \psi + \frac{1}{2G} \sin^2 \psi \\
\varepsilon_{xy} &= \frac{1}{2G'} \sin^2 \psi + \frac{1}{2G} \cos^2 \psi
\end{aligned}
\quad \left. \vphantom{\begin{aligned} \varepsilon_z \\ \varepsilon_{yz} \\ \varepsilon_{xz} \\ \varepsilon_{xy} \end{aligned}} \right\} \begin{array}{l} 2.4 \\ (\text{cont'd}) \end{array}$$

where

- $\sigma_x, \sigma_y, \sigma_z$ = total normal stress components parallel to x-, y-, and z-axes, respectively
- $\sigma_{xz}, \sigma_{yz}, \sigma_{xy}$ = total shearing stress components in xz-, yz-, and xy-planes, respectively
- $\varepsilon_x, \varepsilon_y, \varepsilon_z$ = total normal strain components parallel to x-, y-, and z-axes, respectively
- $\varepsilon_{xz}, \varepsilon_{yz}, \varepsilon_{xy}$ = total shearing strain components in xz-, yz-, and xy-planes, respectively

2.5 FIELD EQUATIONS

In the case of small displacements of a continuous body, the relationships between the components of strain and displacements (Reference 9) are:

$$\left. \begin{aligned} \epsilon_x &= \frac{\partial u}{\partial x}, \quad \epsilon_y = \frac{\partial v}{\partial y}, \quad \epsilon_z = \frac{\partial w}{\partial z} \\ \epsilon_{xz} &= \frac{1}{2} \left(\frac{\partial w}{\partial x} + \frac{\partial u}{\partial z} \right), \quad \epsilon_{yz} = \frac{1}{2} \left(\frac{\partial v}{\partial z} + \frac{\partial w}{\partial y} \right) \\ \epsilon_{xy} &= \frac{1}{2} \left(\frac{\partial u}{\partial y} + \frac{\partial v}{\partial x} \right) \end{aligned} \right\} \quad (2.5)$$

where u , v , and w are the displacements in the x -, y -, and z -directions, respectively.

In the problem under consideration (Figure 2.1), the stresses and displacements are independent of z and become functions of x and y alone. Therefore, Equations 2.5 can be written as:

$$\left. \begin{aligned} \epsilon_x &= \frac{\partial u(x,y)}{\partial x}, \quad \epsilon_y = \frac{\partial v(x,y)}{\partial y}, \quad \epsilon_z = 0 \\ \epsilon_{xz} &= \frac{1}{2} \frac{\partial w(x,y)}{\partial x}, \quad \epsilon_{yz} = \frac{1}{2} \frac{\partial w(x,y)}{\partial y} \\ \epsilon_{xy} &= \frac{1}{2} \left[\frac{\partial u(x,y)}{\partial y} + \frac{\partial v(x,y)}{\partial x} \right] \end{aligned} \right\} \quad (2.6)$$

Equations 2.6 leads to the compatibility equations that guarantee the body is continuous.

The stress components in a continuous body in equilibrium under the action of surface and body forces satisfy three differential equations of equilibrium. In the case under consideration, these equations take the following form:

$$\left. \begin{aligned} \frac{\partial \sigma_x}{\partial x} + \frac{\partial \sigma_{xy}}{\partial y} &= 0 \\ \frac{\partial \sigma_{xy}}{\partial x} + \frac{\partial \sigma_y}{\partial y} &= 0 \\ \frac{\partial \sigma_{xz}}{\partial x} + \frac{\partial \sigma_{yz}}{\partial y} &= 0 \end{aligned} \right\} \quad (2.7)$$

2.6 REPRESENTATION OF THE BOUNDARY CONDITION

Let \bar{X} and \bar{Y} be the x and y components, respectively, of a distributed surface force per unit area; the boundary stress equations (Figure 2.2) can be written as (Reference 9):

$$\left. \begin{aligned} \bar{X} &= \sigma_x \cos(n,x) + \sigma_{xy} \cos(n,y) + \sigma_{xz} \cos(n,z) \\ \bar{Y} &= \sigma_{xy} \cos(n,x) + \sigma_y \cos(n,y) + \sigma_{yz} \cos(n,z) \\ 0 &= \sigma_{xz} \cos(n,x) + \sigma_{yz} \cos(n,y) + \sigma_z \cos(n,z) \end{aligned} \right\} \quad (2.8)$$

For the above equations, the following relationships exist:

$$\left. \begin{aligned} \cos(n,x) &= \frac{dy}{ds} \\ \cos(n,y) &= -\frac{dx}{ds} \\ \cos(n,z) &= 0 \end{aligned} \right\} \quad (2.9)$$

2.7 STRESSES AND DISPLACEMENTS IN CYLINDRICAL COORDINATE SYSTEMS

The relations between the stresses and the displacements in the Cartesian and cylindrical coordinate systems with the same z-axis (Figure 2.1) are:

$$\left. \begin{aligned} \sigma_r &= \sigma_x \cos^2 \theta + \sigma_y \sin^2 \theta + 2\sigma_{xy} \cos \theta \sin \theta \\ \sigma_\theta &= \sigma_x \sin^2 \theta + \sigma_y \cos^2 \theta - 2\sigma_{xy} \cos \theta \sin \theta \\ \sigma_z &= \sigma_z \\ \sigma_{r\theta} &= (\sigma_y - \sigma_x) \cos \theta \sin \theta + \sigma_{xy} (\cos^2 \theta - \sin^2 \theta) \\ \sigma_{rz} &= \sigma_{xz} \cos \theta + \sigma_{yz} \sin \theta \\ \sigma_{\theta z} &= -\sigma_{xz} \sin \theta + \sigma_{yz} \cos \theta \end{aligned} \right\} \quad (2.10)$$

and

$$\left. \begin{aligned} u_r &= u \cos \theta + v \sin \theta \\ v_\theta &= -u \sin \theta + v \cos \theta \end{aligned} \right\} \quad (2.11)$$

where

$$\theta = \tan^{-1} \frac{y}{x} \quad (2.12)$$

and u_r and v_θ are the radial and tangential displacements, respectively. Therefore, if the stresses and the displacements in the xyz coordinate system are known, the corresponding stresses and displacements in the $r\theta z$ coordinate system can easily be obtained.

Table 2.1. Direction cosines.

	x'	y'	z'
x	$\delta_1 = 1$	$\eta_1 = 0$	$\theta_1 = 0$
y	$\delta_2 = 0$	$\eta_2 = \cos \psi$	$\theta_2 = \sin \psi$
z	$\delta_3 = 0$	$\eta_3 = -\sin \psi$	$\theta_3 = \cos \psi$

Table 2.2. Values of q_{ij} in the formulas of transformations (Equation 2.3).

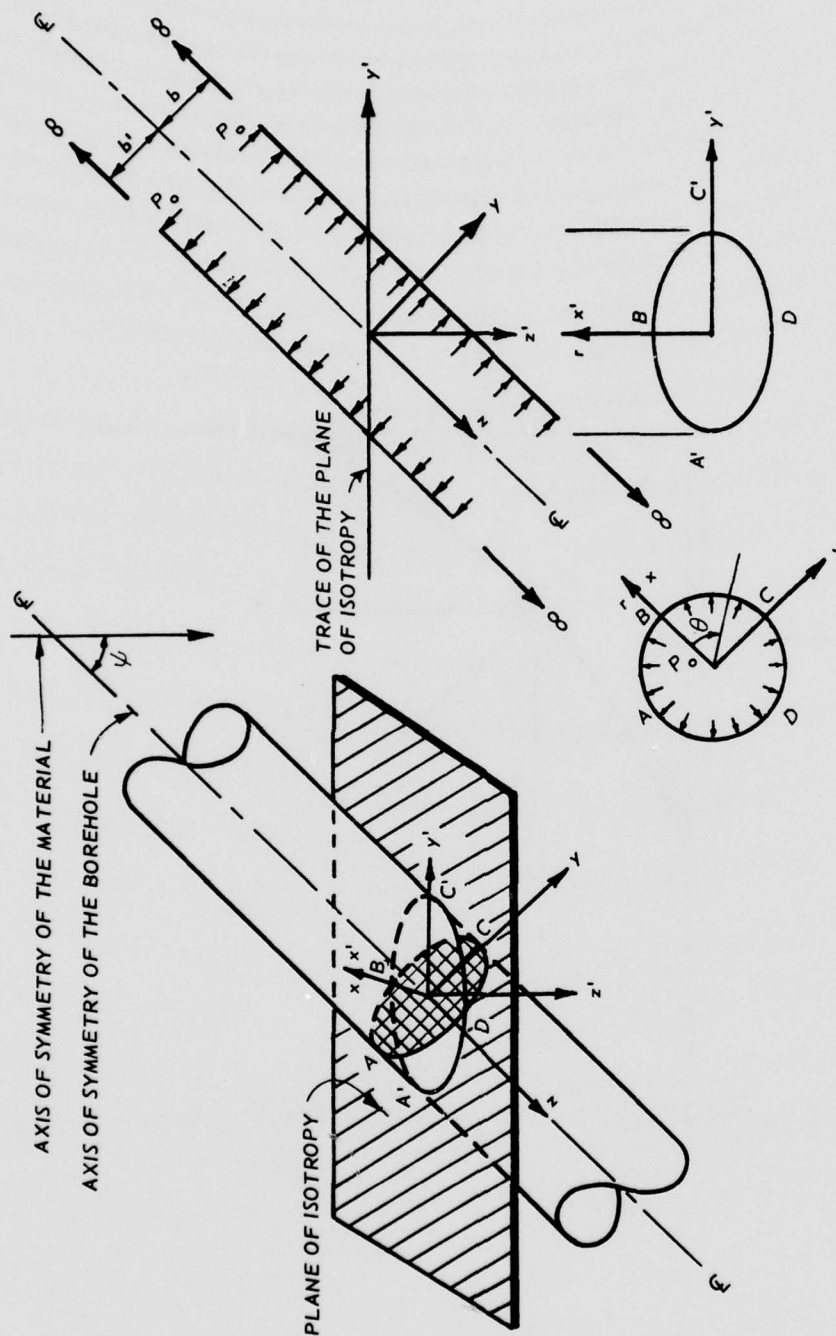
$i \backslash j$	1	2	3	4	5	6
1	δ_1^2	δ_2^2	δ_3^2	$2\delta_2\delta_3$	$2\delta_3\delta_1$	$2\delta_1\delta_2$
2	η_1^2	η_2^2	η_3^2	$2\eta_2\eta_3$	$2\eta_3\eta_1$	$2\eta_1\eta_2$
3	θ_1^2	θ_2^2	θ_3^2	$2\theta_2\theta_3$	$2\theta_3\theta_1$	$2\theta_1\theta_2$
4	$\eta_1\theta_1$	$\eta_2\theta_2$	$\eta_3\theta_3$	$\eta_2\theta_3 + \eta_3\theta_2$	$\eta_1\theta_3 + \eta_3\theta_1$	$\eta_1\theta_2 + \eta_2\theta_1$
5	$\theta_1\delta_1$	$\theta_2\delta_2$	$\theta_3\delta_3$	$\theta_2\delta_3 + \theta_3\delta_2$	$\theta_1\delta_3 + \theta_3\delta_1$	$\theta_1\delta_2 + \theta_2\delta_1$
6	$\delta_1\eta_1$	$\delta_2\eta_2$	$\delta_3\eta_3$	$\delta_2\eta_3 + \delta_3\eta_2$	$\delta_1\eta_3 + \delta_3\eta_1$	$\delta_1\eta_2 + \delta_2\eta_1$

Table 2.3. Value of C'_{ij} from Equation 2.1.

$\begin{array}{c} j \\ i \end{array}$	<u>1</u>	<u>2</u>	<u>3</u>	<u>4</u>	<u>5</u>	<u>6</u>
1	$\frac{1}{E}$	$-\frac{\nu}{E}$	$-\frac{\nu'}{E'}$	0	0	0
2	$-\frac{\nu}{E}$	$\frac{1}{E}$	$-\frac{\nu'}{E'}$	0	0	0
3	$-\frac{\nu'}{E'}$	$-\frac{\nu'}{E'}$	$\frac{1}{E'}$	0	0	0
4	0	0	0	$\frac{1}{G'}$	0	0
5	0	0	0	0	$\frac{1}{G'}$	0
6	0	0	0	0	0	$\frac{1}{G}$

Table 2.4. Value of C_{ij} from Equation 2.3.

$\begin{smallmatrix} j \\ i \end{smallmatrix}$	1	2	3	4	5	6
1	$\frac{1}{E}$	$-\frac{\nu'}{E'} \sin^2 \psi - \frac{\nu}{E} \cos^2 \psi$	$-\frac{\nu'}{E'} \cos^2 \psi - \frac{\nu}{E} \sin^2 \psi$	$\left(\frac{\nu'}{E'} - \frac{\nu}{E}\right) \sin^2 \psi$	0	0
2	$\frac{1}{E}$	$\cos^4 \psi + \frac{1}{E'} \sin^4 \psi$	$-\frac{\nu'}{E'} (\sin^4 \psi + \cos^4 \psi)$	$\left[\left(\frac{1}{E} + \frac{\nu'}{E'}\right) \cos^2 \psi\right.$	0	0
		$\left. + \left(\frac{1}{G'} - \frac{2\nu'}{E'}\right) \cos^2 \psi \sin^2 \psi\right.$	$\left. + \left(\frac{1}{E} + \frac{1}{E'} - \frac{1}{G'}\right) \cos^2 \psi \sin^2 \psi\right.$	$\left. - \left(\frac{1}{E'} + \frac{\nu'}{E'}\right) \sin^2 \psi\right.$		
				$\left. - \frac{1}{2G'} \cos^2 \psi\right] \sin^2 \psi$		
3	S		$\frac{\sin^4 \psi}{E} + \frac{\cos^4 \psi}{E}$	$\left[\left(\frac{1}{E} + \frac{\nu'}{E'}\right) \sin^2 \psi\right.$	0	0
	Y			$\left. - \left(\frac{1}{E'} + \frac{\nu'}{E'}\right) \cos^2 \psi\right.$		
	M		$+ \left(\frac{1}{G'} - \frac{2\nu'}{E'}\right) \cos^2 \psi \sin^2 \psi$	$\left. + \frac{1}{2G'} \cos^2 \psi\right] \sin^2 \psi$		
	M					
	E					
	T					
	R					
4	Y			$\frac{1}{G'}$	0	0
5					$\frac{\cos^2 \psi}{G'} + \frac{\sin^2 \psi}{G}$	0
6						$\frac{\sin^2 \psi}{G'} + \frac{\cos^2 \psi}{G}$



a. THREE-DIMENSIONAL VIEW

b. TWO-DIMENSIONAL VIEW

Figure 2.1 Problem geometry.

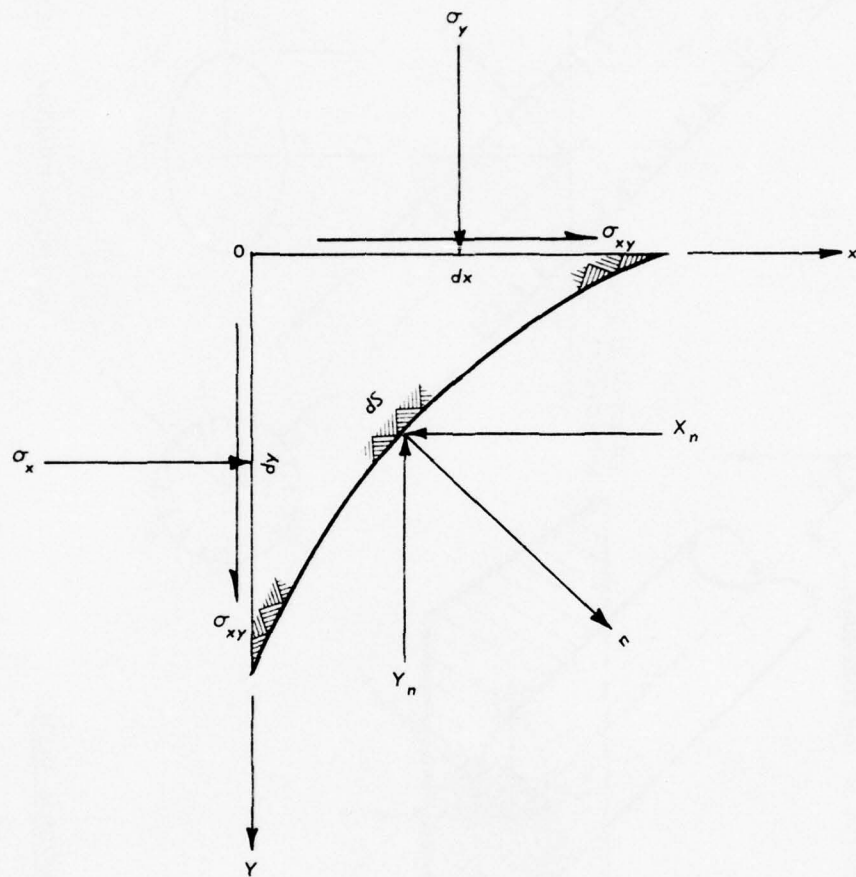


Figure 2.2 Two-dimensional element from the boundary.

CHAPTER 3

DERIVATION OF THE GENERAL SOLUTION OF THE PROBLEM

3.1 GENERAL

The problem of the determination of stresses and displacements around an infinite cylindrical cavity can be formulated analytically by use of the equations presented in Chapter 2. The solution will be unique if it satisfies the equilibrium and compatibility equations and the boundary conditions (Reference 11). This is done below by expressing stresses and displacements as complex harmonic functions in a manner similar to that developed by Lekhnitskii (Reference 9). Recalling Equations 2.4,

$$\left. \begin{aligned} \epsilon_x &= C_{11}\sigma_x + C_{12}\sigma_y + C_{13}\sigma_z + C_{14}\sigma_{yz} \\ \epsilon_y &= C_{12}\sigma_x + C_{22}\sigma_y + C_{23}\sigma_z + C_{24}\sigma_{yz} \\ \epsilon_z &= C_{13}\sigma_x + C_{23}\sigma_y + C_{33}\sigma_z + C_{34}\sigma_{yz} \\ 2\epsilon_{yz} &= C_{14}\sigma_x + C_{24}\sigma_y + C_{34}\sigma_z + C_{44}\sigma_{yz} \\ 2\epsilon_{xz} &= C_{55}\sigma_{xz} \\ 2\epsilon_{xy} &= C_{66}\sigma_{xy} \end{aligned} \right\} \quad (3.1)$$

where the values of C_{ij} are given in Table 2.3. Since $\epsilon_z = 0$ (see Equations 2.6), the third equation of 3.1 leads to

$$\sigma_z = -\frac{1}{C_{33}} (C_{13}\sigma_x + C_{23}\sigma_y + C_{34}\sigma_{yz}) \quad (3.2)$$

Substitution of Equation 3.2 into Equations 3.1, gives

$$\left. \begin{aligned}
 \epsilon_x &= a_{11}\sigma_x + a_{12}\sigma_y + a_{14}\sigma_{yz} \\
 \epsilon_y &= a_{12}\sigma_x + a_{22}\sigma_y + a_{24}\sigma_{yz} \\
 2\epsilon_{yz} &= a_{14}\sigma_x + a_{24}\sigma_y + a_{44}\sigma_{yz} \\
 2\epsilon_{xz} &= a_{55}\sigma_{xz} \\
 2\epsilon_{xy} &= a_{66}\sigma_{xy}
 \end{aligned} \right\} \quad (3.3)$$

in which

$$a_{ij} = c_{ij} - \frac{c_{i3}c_{j3}}{c_{33}} \quad (3.4)$$

Equations 3.3 can be written in terms of the displacements as

$$\left. \begin{aligned}
 \frac{\partial u}{\partial x} &= a_{11}\sigma_x + a_{12}\sigma_y + a_{14}\sigma_{yz} \\
 \frac{\partial v}{\partial y} &= a_{12}\sigma_x + a_{22}\sigma_y + a_{24}\sigma_{yz} \\
 \frac{\partial w}{\partial y} &= a_{14}\sigma_x + a_{24}\sigma_y + a_{44}\sigma_{yz} \\
 \frac{\partial w}{\partial x} &= a_{55}\sigma_{xz} \\
 \frac{\partial u}{\partial y} + \frac{\partial v}{\partial x} &= a_{66}\sigma_{xy}
 \end{aligned} \right\} \quad (3.5)$$

3.2 STRESS FUNCTION

Equations 2.7 (the equilibrium equations) can be satisfied for a homogeneous medium by the introduction of the following stress functions (References 9, 12, and 13):

$$\left. \begin{aligned}
 \sigma_x &= \frac{\partial^2 P(x,y)}{\partial y^2} \\
 \sigma_y &= \frac{\partial^2 P(x,y)}{\partial x^2} \\
 \sigma_{xy} &= - \frac{\partial^2 P(x,y)}{\partial x \partial y} \\
 \sigma_{xz} &= \frac{\partial Q(x,y)}{\partial y} \\
 \sigma_{yz} &= - \frac{\partial Q(x,y)}{\partial x}
 \end{aligned} \right\} \quad (3.6)$$

The compatibility equations can be satisfied by substitution of Equations 3.6 into Equations 3.5 and elimination of u , v , and w by differentiation (Reference 13). Therefore, the following system of differential equations that the stress functions must satisfy can be easily obtained:

$$\left. \begin{aligned}
 L_4 P(x,y) + L_3 Q(x,y) &= 0 \\
 L_3 P(x,y) + L_2 Q(x,y) &= 0
 \end{aligned} \right\} \quad (3.7)$$

where L_2 , L_3 , and L_4 are differential operators of the second, third, and fourth orders, respectively, that have the form:

$$\left. \begin{aligned}
 L_2 &= a_{44} \frac{\partial^2}{\partial x^2} + a_{55} \frac{\partial^2}{\partial y^2} \\
 L_3 &= -a_{24} \frac{\partial^3}{\partial x^3} - a_{14} \frac{\partial^3}{\partial x \partial y^2} \\
 L_4 &= a_{22} \frac{\partial^4}{\partial x^4} + (2a_{12} + a_{66}) \frac{\partial^4}{\partial x^2 \partial y^2} + a_{11} \frac{\partial^4}{\partial y^4}
 \end{aligned} \right\} \quad (3.8)$$

For the components of stresses and displacements around the cylindrical cavity to be continuous and single-valued functions of the coordinates xyz , the stress functions $P(x,y)$ and $Q(x,y)$ must satisfy Equations 3.7 and the boundary conditions.

The general differential equations in terms of $P(x,y)$ and $Q(x,y)$, separately, can be obtained by application of the operator L_2 on the first equation of the system 3.7 and the operator L_3 on the second equation and subtraction of the results. Thus:

$$(L_4 L_2 - L_3^2) P(x,y) = 0 \quad (3.9)$$

Similarly,

$$(L_4 L_2 - L_3^2) Q(x,y) = 0 \quad (3.10)$$

Equations 3.9 and 3.10 are sixth order differential equations where the operator of the sixth order $L_4 L_2 - L_3^2$ can be decomposed into six linear operators of the first order. Hence, Equations 3.9 and 3.10 can be represented in the following forms:

$$\left. \begin{aligned} D_6 D_5 D_4 D_3 D_2 D_1 P(x,y) &= 0 \\ D_6 D_5 D_4 D_3 D_2 D_1 Q(x,y) &= 0 \end{aligned} \right\} \quad (3.11)$$

and

in which

$$D_k = \frac{\partial}{\partial y} - \mu_k \frac{\partial}{\partial x} \quad (k = 1, 2, \dots, 6) \quad (3.12)$$

where μ_k represents the roots of the following algebraic equation that corresponds to the differential Equations 3.9 and 3.10:

$$L_4(\mu) L_2(\mu) - L_3^2(\mu) = 0 \quad (3.13)$$

According to Equations 3.8, $L_2(\mu)$, $L_3(\mu)$, and $L_4(\mu)$ can be written as:

$$\left. \begin{aligned} L_2(\mu) &= a_{55}\mu^2 + a_{44} \\ L_3(\mu) &= -a_{14}\mu^2 - a_{24} \\ L_4(\mu) &= a_{11}\mu^4 + (2a_{12} + a_{66})\mu^2 + a_{22} \end{aligned} \right\} \quad (3.14)$$

Three of the roots of Equation 3.13 are independent; the other three are their complex conjugates (Reference 9).

The integration of Equations 3.9 and 3.10, therefore, can be reduced through Equations 3.11 to the integration of six equations of the first order. The general integral is equal to functions of the arguments

$$\text{and} \quad \left. \begin{aligned} z_k &= x + \mu_k y \\ \overline{z_k} &= x + \overline{\mu_k} y \end{aligned} \right\} \quad (k = 1, 2, 3) \quad (3.15)$$

and can be written as

$$\left. \begin{aligned} P(x, y) &= \sum_{k=1}^{k=3} [P_k(z_k) + \overline{P_k(z_k)}] \\ Q(x, y) &= \sum_{k=1}^{k=3} [Q_k(z_k) + \overline{Q_k(z_k)}] \end{aligned} \right\} \quad (3.16)$$

where $\overline{\mu_k}$ is the complex conjugate of μ_k , $\overline{z_k}$ is the complex conjugate of z_k , and $\overline{P_k(z_k)}$ and $\overline{Q_k(z_k)}$ are the complex conjugates of $P_k(z_k)$ and $Q_k(z_k)$, respectively.

Since the functions $P(x, y)$ and $Q(x, y)$ satisfy Equations 3.7 and 3.8, the following relations between $P(x, y)$ and $Q(x, y)$ exist:

$$Q_k(z_k) = -\frac{L_3(\mu_k)}{L_2(\mu_k)} \frac{dP_k(z_k)}{dz_k} + a_k z_k + b_k \quad (3.17)$$

or

$$Q_k(z_k) = - \frac{L_4(\mu_k)}{L_3(\mu_k)} \frac{dP_k(z_k)}{dz_k} + A_k z_k + B_k \quad (3.18)$$

where a_k , b_k , A_k , and B_k are arbitrary constants. Hence, the stress functions $P(x,y)$ and $Q(x,y)$ (Equations 3.16) can be written as:

$$\begin{aligned} P(x,y) = & P_1(z_1) + \overline{P_1(z_1)} + P_2(z_2) + \overline{P_2(z_2)} \\ & + P_3(z_3) + \overline{P_3(z_3)} \end{aligned} \quad (3.19)$$

$$\begin{aligned} Q(x,y) = & \lambda_1 P'_1(z_1) + \overline{\lambda_1 P'_1(z_1)} + \lambda_2 P'_2(z_2) + \overline{\lambda_2 P'_2(z_2)} \\ & + \frac{1}{\lambda_3} P'_3(z_3) + \overline{\frac{1}{\lambda_3} P'_3(z_3)} + a_k z_k + b_k \end{aligned} \quad (3.20)$$

where

$$\left. \begin{aligned} \lambda_k &= - \frac{L_3(\mu_k)}{L_2(\mu_k)}, \quad (k = 1, 2) \\ \lambda_3 &= - \frac{L_3(\mu_3)}{L_4(\mu_3)} \end{aligned} \right\} \quad (3.21)$$

and

$$P'_k(z_k) = \frac{dP_k}{dz_k}$$

$$P'_k(z_k) = \frac{dP_k(z_k)}{dz_k}$$

Therefore, the general solution to the borehole pressuremeter problem can be completely determined by determining the functions $P_k(z_k)$. But before this can be done, the stresses and the displacements have to be expressed as functions of $P_k(z_k)$.

3.3 COMPLEX REPRESENTATION OF STRESSES AND DISPLACEMENTS

Since the stresses are functions of the second derivative of $P(x,y)$ (Equations 3.6), and the displacements are functions of the first derivative of $P(x,y)$ (Equations 3.5), it is more convenient to introduce the new functions of the complex variable z_k :

$$\left. \begin{aligned} \phi_k(z_k) &= \frac{dP_k(z_k)}{dz_k} = P'_k(z_k) \quad (k = 1, 2) \\ \phi_3(z_3) &= \frac{1}{\lambda_3} \frac{dP_3(z_3)}{dz_3} = \frac{1}{\lambda_3} P'_3(z_3) \end{aligned} \right\} \quad (3.22)$$

With the help of these functions, the expressions for the first and second derivatives of $P(x,y)$ and for the first derivatives of $Q(x,y)$ with respect to x and y may be written in the following way:

$$\begin{aligned} \frac{\partial P(x,y)}{\partial x} &= \phi_1(z_1) + \overline{\phi_1(z_1)} + \phi_2(z_2) + \overline{\phi_2(z_2)} \\ &\quad + \lambda_3 \phi_3(z_3) + \overline{\lambda_3 \phi_3(z_3)} \end{aligned} \quad (3.23)$$

$$\begin{aligned} \frac{\partial^2 P(x,y)}{\partial x^2} &= \phi'_1(z_1) + \overline{\phi'_1(z_1)} + \phi'_2(z_2) + \overline{\phi'_2(z_2)} \\ &\quad + \lambda_3 \phi'_3(z_3) + \overline{\lambda_3 \phi'_3(z_3)} \end{aligned} \quad (3.24)$$

$$\frac{\partial P_k(z_k)}{\partial y} = \frac{dP_k(z_k)}{dz_k} \frac{dz_k}{dy} = \mu_k P'_k(z_k) = \mu_k \phi_k(z_k) \quad (3.25)$$

$$\begin{aligned} \frac{\partial P(x,y)}{\partial y} = & \mu_1 \phi_1(z_1) + \overline{\mu_1 \phi_1(z_1)} + \mu_2 \phi_2(z_2) + \overline{\mu_2 \phi_2(z_2)} \\ & + \mu_3 \lambda_3 \phi_3(z_3) + \overline{\mu_3 \lambda_3 \phi_3(z_3)} \end{aligned} \quad (3.26)$$

$$\begin{aligned} \frac{\partial^2 P(x,y)}{\partial y^2} = & \mu_1^2 \phi_1'(z_1) + \overline{\mu_1^2 \phi_1'(z_1)} + \mu_2^2 \phi_2'(z_2) + \overline{\mu_2^2 \phi_2'(z_2)} \\ & + \mu_3^2 \lambda_3 \phi_3'(z_3) + \overline{\mu_3^2 \lambda_3 \phi_3'(z_3)} \end{aligned} \quad (3.27)$$

$$\begin{aligned} \frac{\partial^2 P(x,y)}{\partial x \partial y} = & \mu_1 \phi_1'(z_1) + \overline{\mu_1 \phi_1'(z_1)} + \mu_2 \phi_2'(z_2) + \overline{\mu_2 \phi_2'(z_2)} \\ & + \mu_3 \lambda_3 \phi_3'(z_3) + \overline{\mu_3 \lambda_3 \phi_3'(z_3)} \end{aligned} \quad (3.28)$$

$$\begin{aligned} Q(x,y) = & \lambda_1 \phi_1(z_1) + \overline{\lambda_1 \phi_1(z_1)} + \lambda_2 \phi_2(z_2) + \overline{\lambda_2 \phi_2(z_2)} \\ & + \phi_3(z_3) + \overline{\phi_3(z_3)} \end{aligned} \quad (3.29)$$

$$\begin{aligned} \frac{\partial Q(x,y)}{\partial x} = & \lambda_1 \phi_1'(z_1) + \overline{\lambda_1 \phi_1'(z_1)} + \lambda_2 \phi_2'(z_2) + \overline{\lambda_2 \phi_2'(z_2)} \\ & + \phi_3'(z_3) + \overline{\phi_3'(z_3)} \end{aligned} \quad (3.30)$$

$$\begin{aligned} \frac{\partial Q(x,y)}{\partial y} = & \mu_1 \lambda_1 \phi_1'(z_1) + \overline{\mu_1 \lambda_1 \phi_1'(z_1)} + \lambda_2 \mu_2 \phi_2'(z_2) + \overline{\lambda_2 \mu_2 \phi_2'(z_2)} \\ & + \mu_3 \phi_3'(z_3) + \overline{\mu_3 \phi_3'(z_3)} \end{aligned} \quad (3.31)$$

According to Equations 3.2 and 3.6, and on the basis of Equations 3.23 through 3.31, the general expression for the components of stresses can be obtained as:

$$\sigma_x = 2\text{Real} \left[\mu_1^2 \phi_1'(z_1) + \mu_2^2 \phi_2'(z_2) + \mu_3^2 \lambda_3 \phi_3'(z_3) \right] \quad (3.32)$$

$$\sigma_y = 2\text{Real} \left[\phi_1'(z_1) + \phi_2'(z_2) + \lambda_3 \phi_3'(z_3) \right] \quad (3.33)$$

$$\sigma_{xy} = -2\text{Real} \left[\mu_1 \phi_1'(z_1) + \mu_2 \phi_2'(z_2) + \mu_3 \lambda_3 \phi_3'(z_3) \right] \quad (3.34)$$

$$\sigma_{xz} = 2\text{Real} \left[\mu_1 \lambda_1 \phi_1'(z_1) + \mu_2 \lambda_2 \phi_2'(z_2) + \mu_3 \phi_3'(z_3) \right] \quad (3.35)$$

$$\sigma_{yz} = -2\text{Real} \left[\lambda_1 \phi_1'(z_1) + \lambda_2 \phi_2'(z_2) + \phi_3'(z_3) \right] \quad (3.36)$$

$$\sigma_z = -\frac{1}{c_{33}} (c_{13} \sigma_x + c_{23} \sigma_y + c_{34} \sigma_{yz}) \quad (3.37)$$

The displacements u , v , and w can be obtained by the substitution of Equations 3.32 through 3.37 into Equations 3.5 and integration of the resulting equations. Thus:

$$\begin{aligned} u = 2\text{Real} \sum_{k=1}^{k=2} \left(a_{11} \mu_k^2 + a_{12} - \lambda_k a_{14} \right) \phi_k(z_k) \\ + 2\text{Real} \left\{ \left[\lambda_3 (a_{11} \mu_3^2 + a_{12}) - a_{14} \right] \phi_3(z_3) \right\} \end{aligned} \quad (3.38)$$

$$\begin{aligned} v = 2\text{Real} \sum_{k=1}^{k=2} \left(a_{12} \mu_k + \frac{a_{22}}{\mu_k} - \frac{\lambda_k}{\mu_k} a_{24} \right) \phi_k(z_k) \\ + 2\text{Real} \left\{ \left[\lambda_3 \left(a_{12} \mu_3 + \frac{a_{22}}{\mu_3} \right) - \frac{a_{24}}{\mu_3} \right] \phi_3(z_3) \right\} \end{aligned} \quad (3.39)$$

$$\begin{aligned} w = 2\text{Real} \sum_{k=1}^{k=2} \left(a_{14} \mu_k + \frac{a_{24}}{\mu_k} - \frac{\lambda_k}{\mu_k} a_{44} \right) \phi_k(z_k) \\ + 2\text{Real} \left\{ \left[\lambda_3 \left(a_{14} \mu_3 + \frac{a_{24}}{\mu_3} \right) - \frac{a_{44}}{\mu_3} \right] \phi_3(z_3) \right\} \end{aligned} \quad (3.40)$$

The stresses and the displacements in cylindrical coordinate systems

can be obtained by substitution of Equations 3.32 through 3.40 into Equations 2.10 and 2.11.

It is clear from Equations 3.32 through 3.40 that $\phi_k(z_k)$ is the only function needed for the determination of stresses and displacements. This function can be determined from the boundary conditions, as shown in the next section.

3.4 DETERMINATION OF THE STRESS FUNCTION

The relationships between the stresses along the boundary and inside the region can be obtained by the combination of Equations 2.8 and Equations 3.32 through 3.37. Thus:

$$\begin{aligned} \phi_1(z_1) + \overline{\phi_1(z_1)} + \phi_2(z_2) + \overline{\phi_2(z_2)} + \lambda_3 \phi_3(z_3) \\ + \overline{\lambda_3 \phi_3(z_3)} = \int_0^S -\bar{Y} ds \quad (3.41) \end{aligned}$$

$$\begin{aligned} \mu_1 \phi_1(z_1) + \overline{\mu_1 \phi_1(z_1)} + \mu_2 \phi_2(z_2) + \overline{\mu_2 \phi_2(z_2)} + \mu_3 \lambda_3 \phi_3(z_3) \\ + \overline{\mu_3 \lambda_3 \phi_3(z_3)} = \int_0^S \bar{X} ds \quad (3.42) \end{aligned}$$

$$\begin{aligned} \lambda_1 \phi_1(z_1) + \overline{\lambda_1 \phi_1(z_1)} + \lambda_2 \phi_2(z_2) + \overline{\lambda_2 \phi_2(z_2)} + \phi_3(z_3) \\ + \overline{\phi_3(z_3)} = C_0 \quad (3.43) \end{aligned}$$

where S is an arc length along the boundary and C_0 is an arbitrary constant.

The arguments, z_k , in the above functions can be written as (see Equation 3.15):

$$z_k = \frac{r}{2} (1 - i\mu_k) \exp(i\theta) + \frac{r}{2} (1 + i\mu_k) \exp(-i\theta) \quad (k = 1, 2, 3) \quad (3.44)$$

where $r = b$ at the boundary and i is a complex number (i.e., $i = 0, 1$).

The function $\phi_k(z_k)$ in the above equations can be considered as functions of the parameter θ having period 2π (References 9 and 13). Hence, Equations 3.41 through 3.43 satisfy Dirichlet conditions and can be expressed by the following two series:

$$\text{Real} [\phi_1(z_1) + \phi_2(z_2) + \lambda_3 \phi_3(z_3)] = \text{Real} \left(\sum_{n=1}^{\infty} \bar{b}_n \frac{e^{-in\theta}}{r^n} \right) \quad (3.45)$$

$$\text{Real} [\mu_1 \phi_1(z_1) + \mu_2 \phi_2(z_2) + \mu_3 \lambda_3 \phi_3(z_3)] = \text{Real} \left(\sum_{n=1}^{\infty} \bar{d}_n \frac{e^{-in\theta}}{r^n} \right) \quad (3.46)$$

$$\text{Real} [\lambda_1 \phi_1(z_1) + \lambda_2 \phi_2(z_2) + \phi_3(z_3)] = \text{Real} (C_0) \quad (3.47)$$

A comparison between Equations 3.41 through 3.43 and 3.45 through 3.47 leads to

$$\int_0^S -\bar{Y} dS = b \int_0^\theta -\bar{Y} d\theta = \sum_{n=1}^{\infty} \left(b_n \frac{e^{in\theta}}{b^n} + \bar{b}_n \frac{e^{-in\theta}}{b^n} \right) \quad (3.48)$$

$$\int_0^S \bar{X} dS = b \int_0^\theta \bar{X} d\theta = \sum_{n=1}^{\infty} \left(d_n \frac{e^{in\theta}}{b^n} + \bar{d}_n \frac{e^{-in\theta}}{b^n} \right) \quad (3.49)$$

The coefficients b_n and d_n can be obtained by use of the properties of the Fourier series (Reference 13) and the problem geometry defined in Section 2.2, which yield the following values:

$$\bar{b}_1 = -\frac{P_0 b^2}{2}, \quad \bar{d}_1 = -\frac{P_0 b^2 i}{2} \quad (3.50)$$

$$b_n = d_n = 0 \quad \text{for } n \geq 2$$

Substitution of Equations 3.50 into Equations 3.45 through 3.47 leads to:

$$\text{Real} [\phi_1(z_1) + \phi_2(z_2) + \lambda_3 \phi_3(z_3)] = \text{Real} \left(-\frac{P_o b^2}{2r} e^{-i\theta} \right) \quad (3.51)$$

$$\text{Real} [\mu_1 \phi_1(z_1) + \mu_2 \phi_2(z_2) + \mu_3 \lambda_3 \phi_3(z_3)] = \text{Real} \left(\frac{-P_o b^2 i}{2r} e^{-i\theta} \right) \quad (3.52)$$

$$\text{Real} [\lambda_1 \phi_1(z_1) + \lambda_2 \phi_2(z_2) + \phi_3(z_3)] = 0 \quad (3.53)$$

When Equations 3.51 through 3.53 are solved, this results:

$$\phi_1(z_1) = \frac{P_o b^2}{2r} \left[\frac{(\mu_3 \lambda_2 \lambda_3 - \mu_2) + (1 - \lambda_2 \lambda_3) i}{\mu_2 - \mu_1 + \lambda_2 \lambda_3 (\mu_1 - \mu_3) + \lambda_1 \lambda_3 (\mu_3 - \mu_2)} \right] \exp(-i\theta) \quad (3.54)$$

$$\phi_2(z_2) = \frac{P_o b^2}{2r} \left[\frac{(\mu_1 - \mu_3 \lambda_1 \lambda_3) + (\lambda_1 \lambda_3 - 1) i}{\mu_2 - \mu_1 + \lambda_2 \lambda_3 (\mu_1 - \mu_3) + \lambda_1 \lambda_3 (\mu_3 - \mu_2)} \right] \exp(-i\theta) \quad (3.55)$$

$$\phi_3(z_3) = \frac{P_o b^2}{2r} \left[\frac{(\mu_2 \lambda_1 - \mu_1 \lambda_2) + (\lambda_2 - \lambda_1) i}{\mu_2 - \mu_1 + \lambda_2 \lambda_3 (\mu_1 - \mu_3) + \lambda_1 \lambda_3 (\mu_3 - \mu_2)} \right] \exp(-i\theta) \quad (3.56)$$

The derivative of the functions ϕ_k can be easily obtained from the above equations:

$$\begin{aligned} \phi_1'(z_1) = \frac{P_o b^2}{2r^2} \left[\frac{(\mu_3 \lambda_2 \lambda_3 - \mu_2) + (1 - \lambda_2 \lambda_3) i}{\mu_2 - \mu_1 + \lambda_2 \lambda_3 (\mu_1 - \mu_3) + \lambda_1 \lambda_3 (\mu_3 - \mu_2)} \right] \\ \times \left(\frac{\sin \theta + i \cos \theta}{\sin \theta - \mu_1 \cos \theta} \right) \quad (3.57) \end{aligned}$$

$$\phi'_2(z_2) = \frac{P_o b^2}{2r^2} \left[\frac{(\mu_1 - \mu_3 \lambda_1 \lambda_3) + (\lambda_1 \lambda_3 - 1) i}{\mu_2 - \mu_1 + \lambda_2 \lambda_3 (\mu_1 - \mu_3) + \lambda_1 \lambda_3 (\mu_3 - \mu_2)} \right] \times \left(\frac{\sin \theta + i \cos \theta}{\sin \theta - \mu_2 \cos \theta} \right) \quad (3.58)$$

$$\phi'_3(z_3) = \frac{P_o b^2}{2r^2} \left[\frac{(\mu_2 \lambda_1 - \mu_1 \lambda_2) + (\lambda_2 - \lambda_1) i}{\mu_2 - \mu_1 + \lambda_2 \lambda_3 (\mu_1 - \mu_3) + \lambda_1 \lambda_3 (\mu_3 - \mu_2)} \right] \times \left(\frac{\sin \theta + i \cos \theta}{\sin \theta - \mu_3 \cos \theta} \right) \quad (3.59)$$

The distribution of stresses can be determined from Equations 2.10, 3.32 through 3.37 and 3.57 through 3.59, and the distribution of displacements can be determined from Equations 2.11, 3.38 through 3.40, and 3.54 through 3.56. The computer program BOREHOLE was developed to solve numerically the above system of equations and to generate various plots of stress and displacement distributions around the cylindrical cavity. Examples of the distribution of stresses and displacements are given in Figures 3.1 through 3.8.

The volume change of a unit length along the generator of the borehole can be obtained from the radial displacement (Equation 3.38) at $r = b$, and $\theta = 0$, and $\theta = \pi/2$:

$$\frac{\Delta V}{V} = \frac{\pi [b + u(b, 0)] \left[b + u\left(b, \frac{\pi}{2}\right) \right] - \pi b^2}{\pi b^2}$$

or

$$\frac{\Delta V}{V} = \frac{u(b, 0) + u\left(b, \frac{\pi}{2}\right)}{b} + \frac{u(b, 0) u\left(b, \frac{\pi}{2}\right)}{b^2} \quad (3.60)$$

Equation 3.60 is a function of the five material properties as well as the angle of inclination of the borehole, ψ (Figure 2.1).

Therefore, the solution of Equation 3.60 for the material properties is not straightforward and requires an iterative scheme and a large computer program such as BOREHOLE. However, the solution is relatively simple if four material properties as well as the volume change are known.

In the following section, spatial stress and displacement distributions for a sample problem are investigated. The material properties used in this sample problem as well as the angle of inclination of the borehole are tabulated below.

<u>E</u>	<u>E'</u>	<u>ν</u>	<u>ν'</u>	<u>G'</u>	<u>G</u>	<u>ψ</u>	<u>r_o</u>	<u>P</u>
ksi	ksi			ksi	ksi	degree	inch	ksi
7.8	2.6	0.3	0.2	1.5	3.0	30	1.5	1.0

3.5 SPATIAL STRESS DISTRIBUTION FOR SAMPLE PROBLEM

Figure 3.1 shows a typical result of the radial and tangential stresses along the radius for $\theta = 0$ degrees¹ (Figure 2.1) at an angle of inclination of 30 degrees. The solid line shows the radial stress while the dashed line shows the tangential stress.

Figure 3.2 shows a radial stress contour in dimensionless form, σ_r/P_o , at an angle of inclination of 30 degrees. It is clear from this figure that the radial stress attenuates to a value of $\sigma_r/P_o = 0.25$ at $r = 2r_o$.

The distribution of tangential stress along the boundary of the borehole whose angle of inclination is 30 degrees is shown in Figure 3.3.

Figure 3.4 shows the distribution of radial and shear stresses along the boundary of the borehole whose angle of inclination is 30 degrees. It is interesting to note that the shear stress, $\sigma_{\theta z}$, along the boundary of the borehole is not zero but would be if the material were isotropic.

¹ A table of factors for converting U. S. customary units of measurement to metric (SI) units is presented on page 2.

3.6 SPATIAL DISPLACEMENT DISTRIBUTION FOR SAMPLE PROBLEM

Figure 3.5 shows a typical result of the radial displacements along the radius of the borehole for $\theta = 0$ and 90 degrees at an angle of inclination of 30 degrees. The solid line shows the radial displacement for $\theta = 90$ degrees and the dashed line shows the radial displacement for $\theta = 0$ degrees. Note that both the solid and the dashed lines would coincide if the material is isotropic.

Figure 3.6 shows a radial displacement contour in dimensionless form $u_r/u_r(r_0)$, at an angle of inclination of 30 degrees where u_r is the radial displacement at r and θ , and $u_r(r_0)$ is the radial displacement along the boundary of the borehole. It is clear from Figures 3.5 and 3.6 that for this case approximately one half of the borehole volume change is due to strains in the material within one borehole-radius of the sidewall. It is also clear that three fourths of the borehole volume change is due to strains that occur at less than three radii from the borehole sidewall. Since the radius of a borehole pressuremeter test is typically 1.5 inches, only a very small volume of in situ material close to the borehole can significantly influence the test results.

The distribution of the radial and tangential displacements along the boundary of the borehole whose angle of inclination is 30 degrees is shown in Figure 3.7. As the figure shows, the borehole deforms to an elliptical shape under load.

Figure 3.8 shows a tangential displacement contour in dimensionless form $v_\theta/v_\theta(r_0)$ where v_θ is the tangential displacement at r and θ , and $v_\theta(r_0)$ is the tangential displacement along the boundary of the borehole.

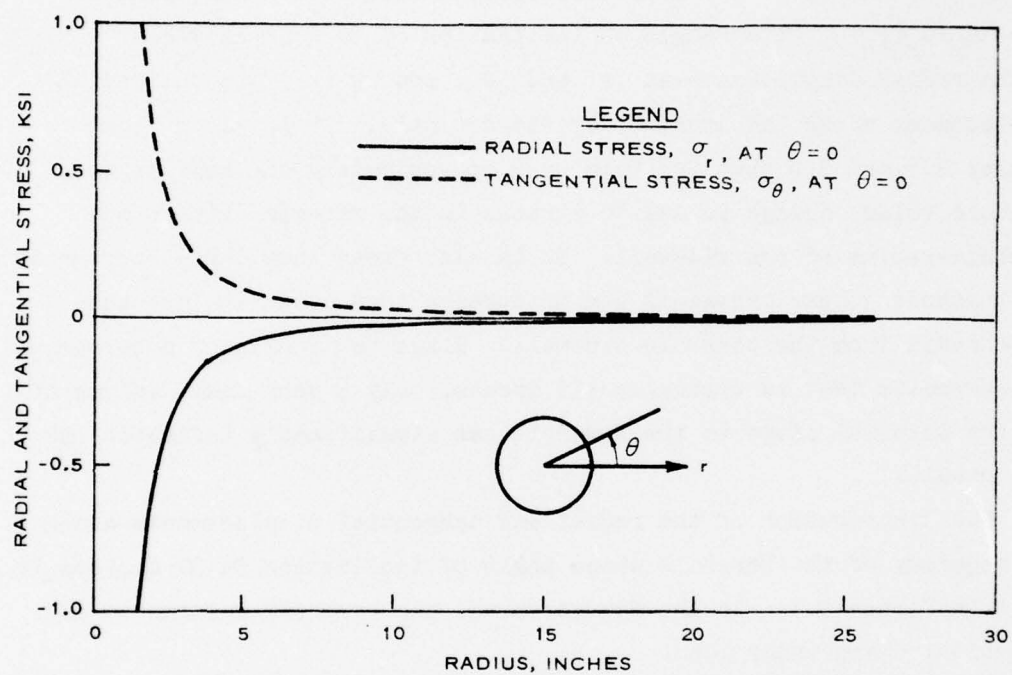


Figure 3.1 Distribution of radial and tangential stresses along the radius for $\theta = 0$ degrees at an angle of inclination of 30 degrees.

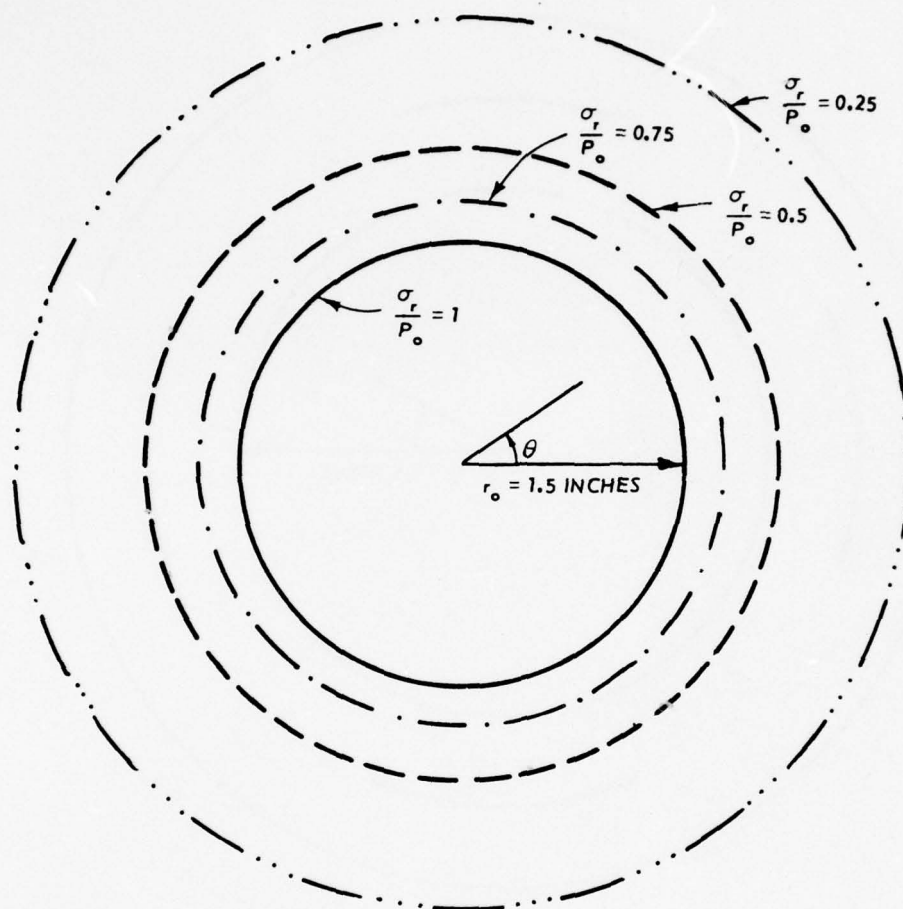


Figure 3.2 Contour for radial stress at an angle of inclination of 30 degrees.

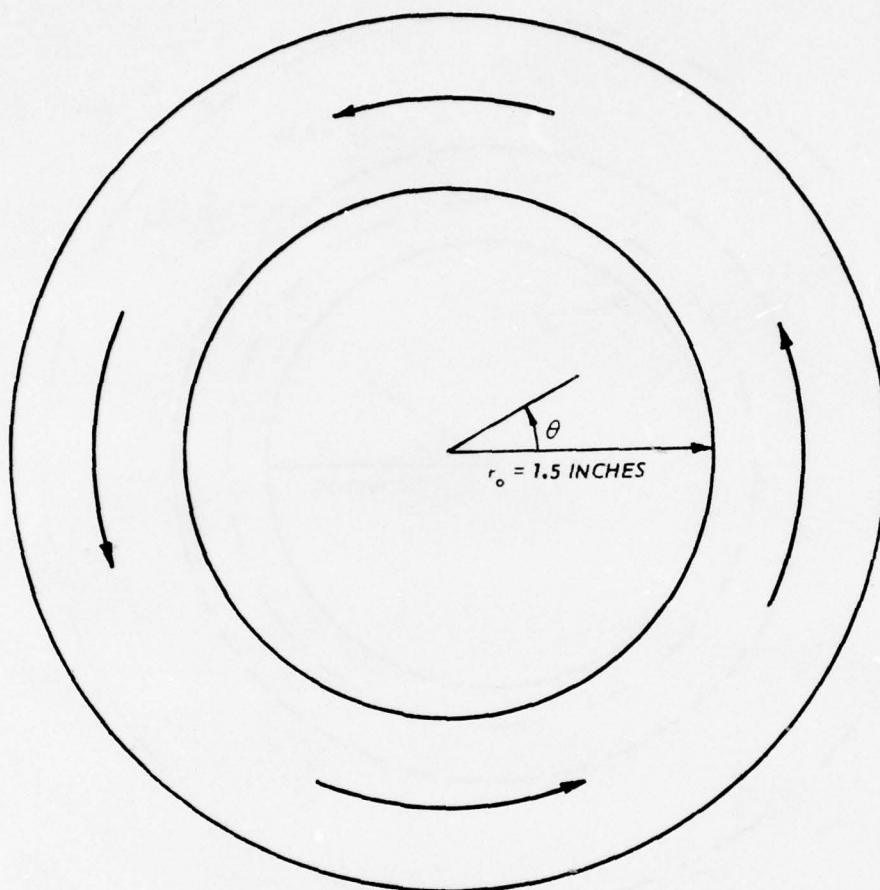


Figure 3.3 Distribution of tangential stress along the boundary of the borehole whose angle of inclination is 30 degrees.

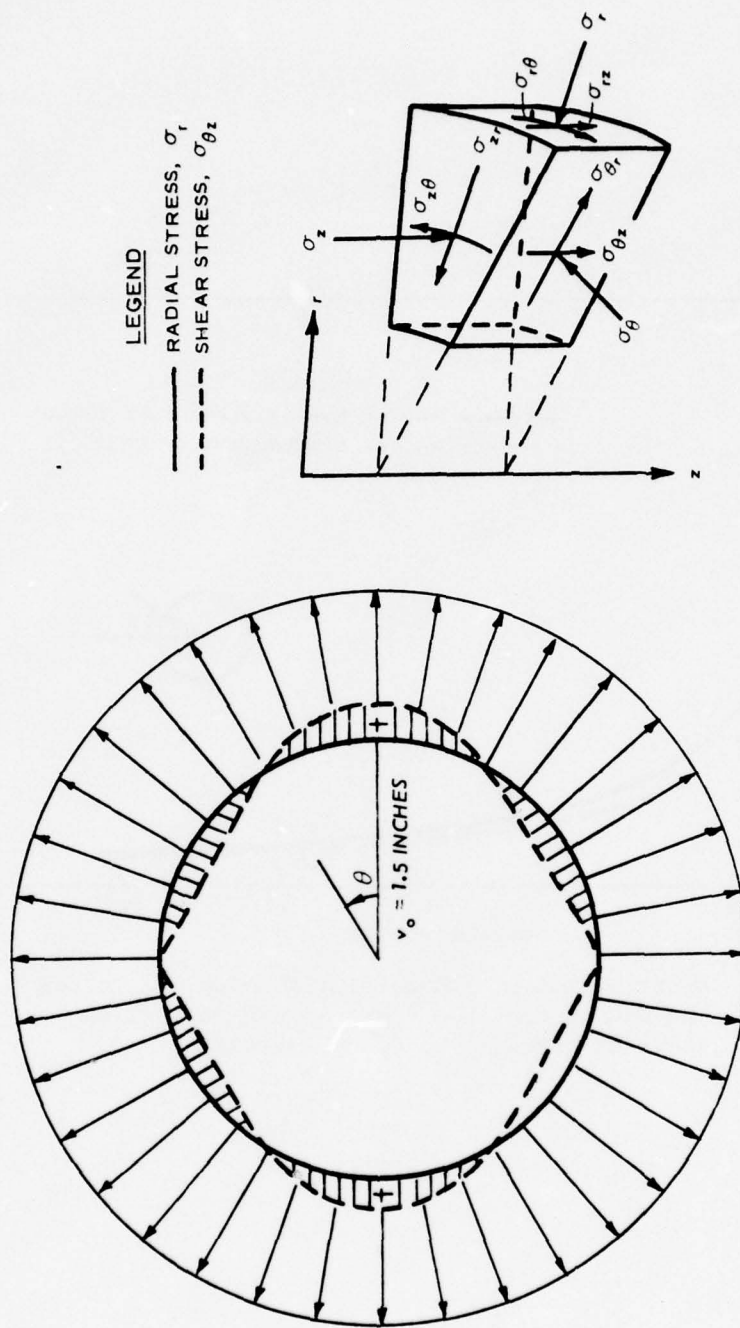


Figure 3.4 Distribution of radial and shear stresses along the boundary of the borehole whose angle of inclination is 30 degrees.

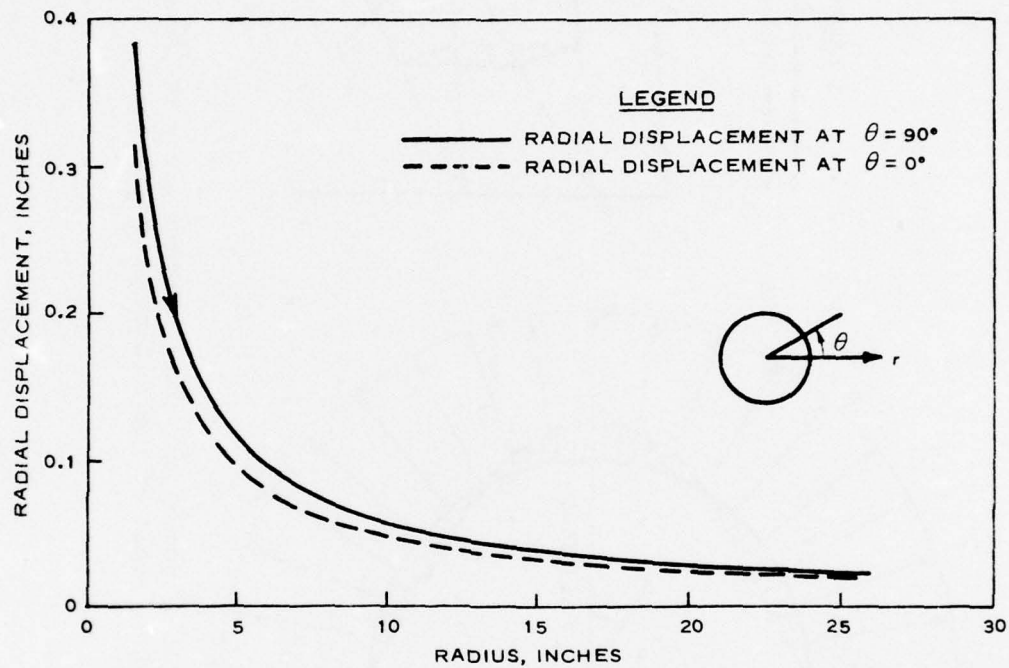


Figure 3.5 Distribution of radial displacement u_r along the radius for $\theta = 0$ and 90 degrees at an angle of inclination of 30 degrees.

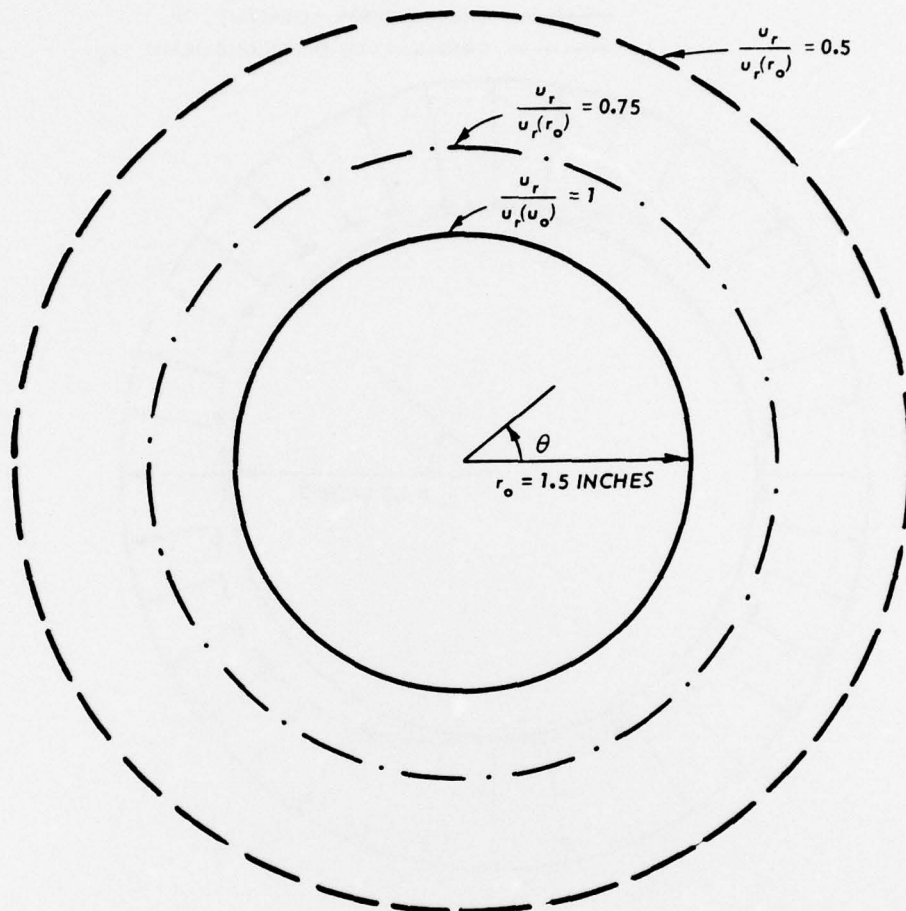


Figure 3.6 Contour for radial displacement at an angle of inclination of 30 degrees.

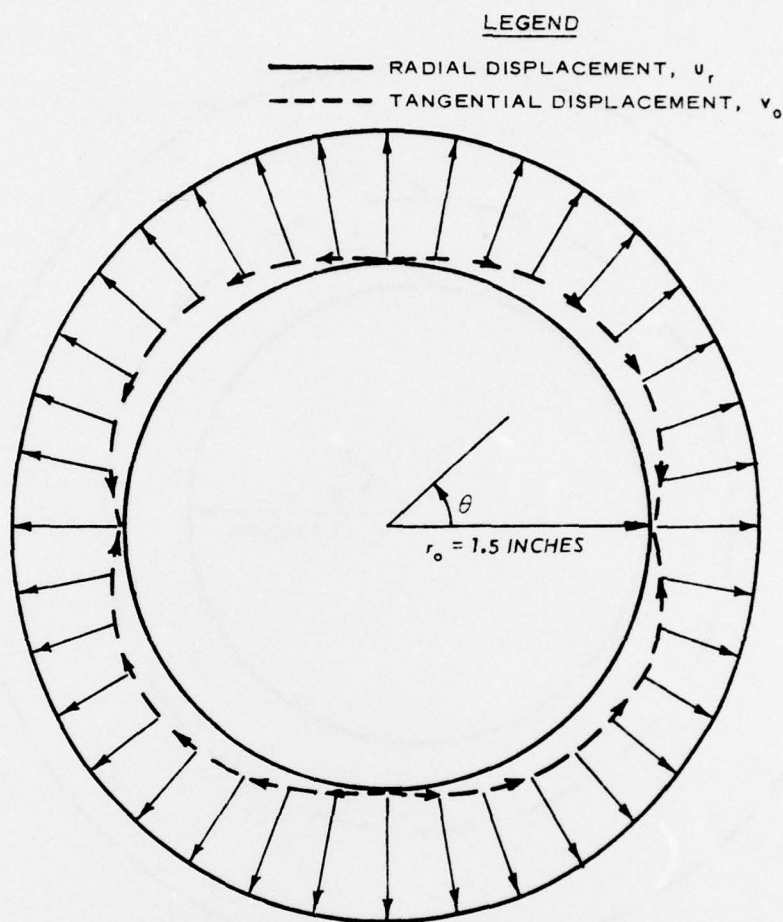


Figure 3.7 Distribution of radial and tangential displacements along the boundary of the borehole whose angle of inclination is 30 degrees.

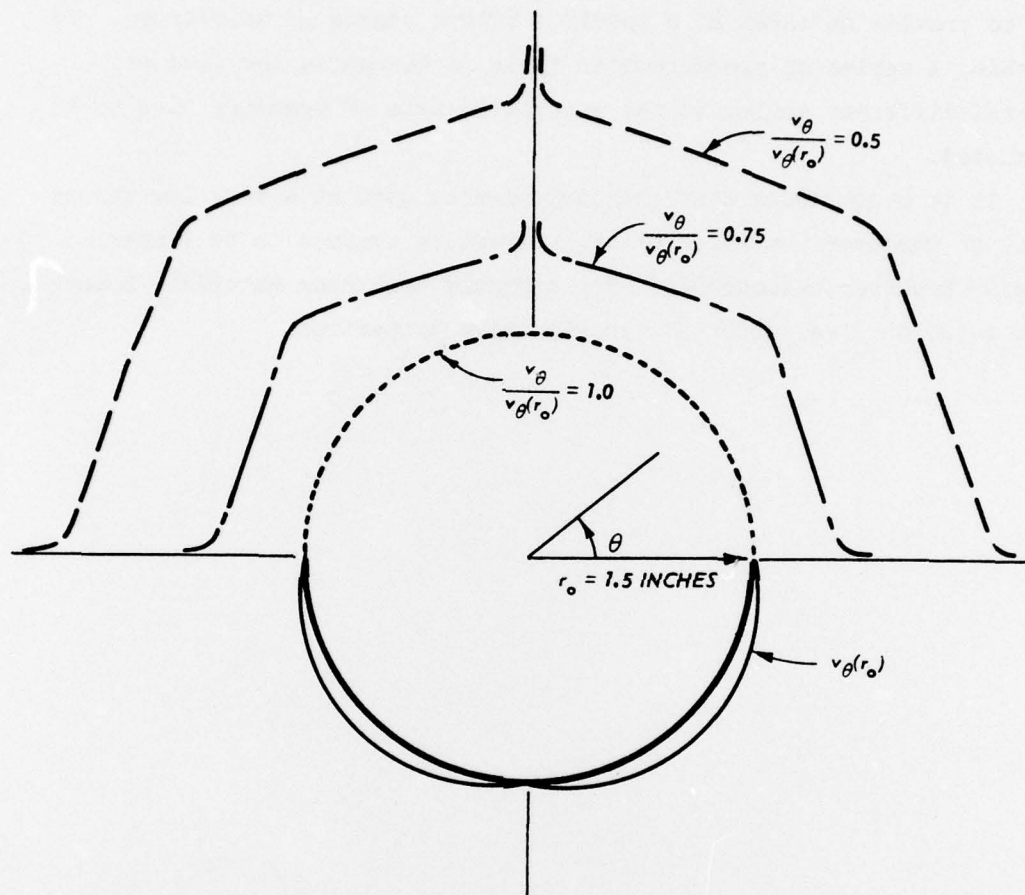


Figure 3.8 Contour for tangential displacement at an angle of inclination of 30 degrees.

CHAPTER 4

CONCLUSIONS AND RECOMMENDATIONS

The solution presented herein can be used in the analysis of borehole pressuremeter test data to provide an appropriate set of linear elastic transverse-isotropic constitutive properties for a given medium and to provide an index of a specific site's degree of anisotropy. To do this, a series of pressuremeter tests in boreholes inclined at several different angles to the material's axis of symmetry have to be conducted.

It is recommended that this solution be used at a very low stress level or whenever the material of interest is assumed to be linear elastic transverse-isotropic. For a highly nonlinear material, however, this solution gives effective constitutive properties.

REFERENCES

1. L. E. Menard; "An Apparatus for Measuring the Strength of Soils in Place"; Thesis; 1957; University of Illinois, Urbana, Ill.
2. L. Ménard; "Mesures In Situ des Propriétés Physiques des Sols"; *Annals des Ponts et Chaussées*, Vol 127, No. 3, 1957, pp 357-377.
3. L. Ménard; "Influence de L'amplitude et de L'historie d'un Champ de Contraintes sur le Tassement d'un sol de Fondation"; Proceedings, 5th International Conference on Soil Mechanics, Paris, 1961, pp 249-253.
4. J. B. Palmerton and J. B. Warriner; "Postshot In Situ Material Property Tests at the Mixed Company Site, Colorado"; Miscellaneous Paper S-74-8, May 1974; U. S. Army Engineer Waterways Experiment Station, CE, Vicksburg, Miss.
5. J. B. Palmerton; "Menard Pressuremeter Tests at FRENCHMAN FLAT, Nevada Test Site"; WES (WESSD) Technical Letter; October 1973; U. S. Army Engineer Waterways Experiment Station, CE, Vicksburg, Miss.
6. J. B. Palmerton; "Menard Pressuremeter Tests at YUCCA LAKE, Nevada Test Site"; WES (WESSD) Technical Letter; October 1973; U. S. Army Engineer Waterways Experiment Station, CE, Vicksburg, Miss.
7. J. B. Warriner; "Project MIDDLE GUST: Postshot Borehole Pressuremeter Tests and Sample Determination Experiments"; WES (WESSD) Technical Letter; June 1975; U. S. Army Engineer Waterways Experiment Station, CE, Vicksburg, Miss.
8. G. Y. Baladi; "An Elastic-Plastic Constitutive Relation for Transverse-Isotropic Three-Phase Earth Material"; Miscellaneous Paper (in publication); U. S. Army Engineer Waterways Experiment Station, CE, Vicksburg, Miss.
9. S. G. Lekhnitskii; "Theory of Elasticity of an Anisotropic Elastic Body"; 1963; Holden-Day, San Francisco.
10. R. E. Gibson and W. F. Anderson; "In-Situ Measurements of Soil Properties with the Pressuremeter"; *Civil Engineering Public Works Rev.* 56, No. 658, 1963, pp 615-618.
11. V. V. Novozhilov; "Theory of Elasticity"; 1961; Pergaman Press, New York.
12. S. Timoshenko and J. N. Goodier; "Theory of Elasticity"; 2nd ed.; 1951; McGraw-Hill, New York.
13. N. I. Muskhelishvili; "Some Basic Problems of the Mathematical Theory of Elasticity"; 1963; Noordhoff, Groningen.

APPENDIX A: NOTATION

a_{ij}	Material properties matrix
a_k, b_k, A_k, B_k	Arbitrary constants
b	Radius of the cylindrical cavity
C_{ij}	Elastic properties for the coordinate system xyz
C'_{ij}	Elastic properties for the coordinate system $x'y'z'$
C_o	Arbitrary constant
D_k	Complex operator
E	Young's modulus in the plane of isotropy
E'	Young's modulus in a plane normal to the plane of isotropy
G	Shear modulus for the plane of isotropy
G'	Shear modulus for a plane normal to the plane of isotropy
L_2, L_3, L_4	Differential operators of the second, third, and fourth orders, respectively
$L_4 L_2 - L_3$	Differential operator of the sixth order
$P_k(z_k)$	Complex stress function
$\overline{P_k(z_k)}$	Complex conjugate of $P_k(z_k)$
P_o	Applied load on the boundary of the borehole
$P(x,y)$	Stress function
q_{ij}	Transformation matrix for this appears in Equation 2.3
$Q_k(z_k)$	Complex stress function
$\overline{Q_k(z_k)}$	Complex conjugate of $Q_k(z_k)$
$Q(x,y)$	Stress function
$r\theta z$	Cylindrical coordinate system
S	Arc length along the boundary
u_r	Radial displacement
$u_r(r_o)$	Radial displacement along the boundary of the borehole
u,v,w	Displacements in the x -, y -, and z -directions, respectively
v_o	Initial volume of a unit length of the borehole

v_{θ}	Tangential displacement
$v_{\theta}(r_o)$	Tangential displacement along the boundary of the borehole
xyz	Cartesian coordinate system in which the solution of the borehole pressuremeter problem is solved
$x'y'z'$	Cartesian coordinate system in which $x'y'$ is parallel to the plane of isotropy
\bar{X}	The x component of a distributed surface force per unit area
\bar{Y}	The y component of a distributed surface force per unit area
z_k	Complex plane
$\overline{z_k}$	Complex conjugate of z_k
ΔV	Change in volume per unit length of a borehole
$\epsilon_x, \epsilon_y, \epsilon_z$	Total normal strain components parallel to x-, y-, and z-axes, respectively
$\epsilon_{x'}, \epsilon_{y'}, \epsilon_{z'}$	Total normal strain components parallel to x'-, y'-, and z'-axes, respectively
$\epsilon_{xz}, \epsilon_{yz}, \epsilon_{xy}$	Total shearing strain components in xz-, yz-, and xy-planes, respectively
$\epsilon_{x'z'}, \epsilon_{y'z'}, \epsilon_{x'y'}$	Total shearing strain components in x'z'-, y'z'-, and x'y'-planes, respectively
u_k	Root of the algebraic equation that corresponds to differential Equations 3.9 and 3.10
ν	Poisson's ratio that characterizes the transverse reduction in the plane of isotropy due to stress in the same plane
ν'	Poisson's ratio that characterizes the transverse reduction in the plane of isotropy due to stress normal to it
σ_r	Radial stress
$\sigma_x, \sigma_y, \sigma_z$	Total normal stress components parallel to the x-, y-, and z-axes, respectively
$\sigma_{x'}, \sigma_{y'}, \sigma_{z'}$	Total normal stress components parallel to the x'-, y'-, and z'-axes, respectively
$\sigma_{xz}, \sigma_{yz}, \sigma_{xy}$	Total shearing stress components in xz-, yz-, and xy-planes, respectively
$\sigma_{x'z'}, \sigma_{y'z'}, \sigma_{x'y'}$	Total shearing stress components in x'z'-, y'z'-, and x'y'-planes, respectively

σ_{θ} Tangential stress
 $\sigma_{\theta z}$ Shear stress in θz plane
 ψ Angle of inclination of the borehole

DISTRIBUTION LIST

Address	No. of Copies
<u>DOD</u>	
Defense Documentation Center, Cameron Station, Alexandria, Virginia 22314 ATTN: TC/Mr. Meyer B. Kahn	2
Director, Defense Advanced Research Projects Agency, 1400 Wilson Blvd., Arlington, Virginia 22209 ATTN: Technical Library	1
Director of Defense Research and Engineering, Washington, D. C. 20301 ATTN: Technical Library, Room 3C-128	1
Director, Defense Nuclear Agency, Washington, D. C. 20305 ATTN: SPSS TITL	3 2
Director, Defense Communications Agency, Washington, D. C. 20305 ATTN: Technical Library	1
<u>Army</u>	
Headquarters, Department of the Army, Washington, D. C. 20314 ATTN: DAEN-ASI-L DAEN-MCE-D/D. S. Reynolds DAEN-RDL	2 1 1
Division Engineer, U. S. Army Engineer Division, Huntsville Huntsville, Alabama 35807 ATTN: HNDED-SR/Mr. Charles L. Huang	1
Division Engineer, U. S. Army Engineer Division, Missouri River, P. O. Box 103, Downtown Station, Omaha, Nebraska 68101 ATTN: Library	1
Commander/Director, U. S. Army Cold Regions Research and Engineering Laboratory, P. O. Box 282, Hanover, New Hampshire 03755 ATTN: Technical Library	1

Address	No. of Copies
<u>Army (Continued)</u>	
U. S. Military Academy, Department of Engineering, West Point, New York 10996 ATTN: Course Director, Soil Mechanics	1
Director, U. S. Army Construction Engineering Research Laboratory, P. O. Box 4005, Champaign, Illinois 61820 ATTN: Library	1
Commander, U. S. Army Materiel Development and Readiness Command (DARCOM), 5001 Eisenhower Avenue, Alexandria, Virginia 22333 ATTN: Technical Library	1
District Engineer, U. S. Army Engineer District, Ohio River, P. O. Box 1159, Cincinnati, Ohio 45201 ATTN: Library	1
<u>Navy</u>	
Officer in Charge, Civil Engineering Laboratory, Naval Construction Battalion Center, Port Hueneme, California 93043 ATTN: Technical Library (Code L08A)	1
Commander, Naval Facilities Engineering Command, San Bruno, California 94066 ATTN: Technical Library	1
<u>Air Force</u>	
Commander, Space and Missile Systems Organization, Norton Air Force Base, California 92409 ATTN: MNNH/MAJ D. H. Gage MNNH/CPT J. V. Kaiser, Jr.	1 1
Commander, Air Force Weapons Laboratory, Kirtland Air Force Base, New Mexico 87117 ATTN: DES-G/L. S. Melzer DES-C/CPT G. W. Ullrich	1 1
Deputy Chief of Staff for Research and Development, Headquarters, U. S. Air Force, Washington, D. C. 20702 ATTN: AFRD/Technical Library	1

Address	No. of Copies
<u>Air Force (Continued)</u>	
Air Force Institute of Technology, AFIT Bldg 640, Area B, Wright-Patterson Air Force Base, Ohio 45433 ATTN: Technical Library	1
<u>Other Government Agencies</u>	
Director, Lawrence Livermore Laboratory, Technical Information Division, P. O. Box 808, Livermore, California 94550 ATTN: Technical Library	1
Sandia Laboratories, P. O. Box 5800, Albuquerque, New Mexico 87115 ATTN: Library	1
Director, Los Alamos Scientific Laboratory, P. O. Box 1663, Los Alamos, New Mexico 87544 ATTN: Library	1
Bureau of Mines, Denver Federal Center, Building 20, Denver, Colorado 80225 ATTN: Technical Library	1
Nuclear Regulatory Commission, Directorate of Licensing Regulations, Washington, D. C. 20545 ATTN: Site Analysis Branch/Dr. Lyman Heller	1
<u>Others</u>	
University of Illinois, Civil Engineering Building, Urbana, Illinois 61801 ATTN: Prof. W. J. Hall Prof. A. J. Hendron, Jr.	1 1
University of New Mexico, Civil Engineering Research Facility, P. O. Box 188, University Station, Albuquerque, New Mexico 87106 ATTN: Mr. C. J. Higgins	1
Texas A&M University, Center of Tectonophysics, College Station, Texas 77843 ATTN: Dr. John Handin, Director	1
Agbabian Associates, Engineering Consultants, 250 N. Nash Street, El Segundo, California 90245	1

Address	No. of Copies
<u>Others (Continued)</u>	
Applied Theory Incorporated, 1010 Westwood Blvd., Los Angeles, California 90024 ATTN: Dr. John G. Trulio	1
California Research and Technology, Inc., 6269 Variel Avenue, Woodland Hills, California 91364 ATTN: Technical Library	1
General Electric Company, TEMPO, 816 State Street, Santa Barbara, California 93102 ATTN: Mr. Warren Chan (DASIAC)	1
Merritt Cases, Inc., P. O. Box 1206, Redlands, California 92373 ATTN: J. L. Merritt	1
Pacifica Technology, P. O. Box 148, Del Mar, California 92014 ATTN: Technical Library	1
Physics International Company, 2700 Merced Street, San Leandro, California 94577 ATTN: Mr. Dennis Orphal	1
R&D Associates, P. O. Box 9695, Marina Del Rey, California 90291 ATTN: Dr. H. F. Cooper, Jr. Mr. R. J. Port	1 1
TRW Defense and Space Systems Group, Maie Station R1/2178, Redondo Beach, California 90278 ATTN: Mr. Norman Lipner	1
Weidlinger Associates, Consulting Engineers, 110 E. 59th, New York, New York 10022 ATTN: Dr. Melvin L. Baron Dr. Ivan S. Sandler	1 1
Stanford Research Institute, 333 Ravenswood Avenue, Menlo Park, California 94025 ATTN: Technical Library	1
Terra Tek, University Research Park, 420 Wakara Way, Salt Lake City, Utah 84108 ATTN: Dr. A. S. Abou-sayed Dr. H. R. Pratt	1 1

<u>Address</u>	<u>No. of Copies</u>
<u>Others (Continued)</u>	
Science Applications, Inc., Suite 216, 2201 San Pedro, N.E. Albuquerque, New Mexico 87110 ATTN: Mr. J. L. Bratton	1
Weidlinger Associates, Consulting Engineers, 3000 Sand Hill Road, Suite 245, Menlo Park, California 99025 ATTN: Dr. Jeremy Isenberg	1
Fugro National, Inc., P. O. Box 7765, Long Beach, California 90807 ATTN: Mr. Ken Wilson	1
Shannon and Wilson, Inc., 1105 N. 38th Street, Seattle, Washington 98103 ATTN: Mr. Earl A. Sibley	1
Duke University, Department of Engineering, Durham, North Carolina 27706 ATTN: Prof. A. B. Vesic	1
Georgia Institute of Technology, School of Civil Engineering, Atlanta, Georgia 30332 ATTN: Dr. B. B. Mazanti	1
University of Michigan, Department of Civil Engineering, 304 West Engineering, Ann Arbor, Michigan 48104 ATTN: Prof. F. E. Richart, Jr.	1
Massachusetts Institute of Technology, 77 Massachusetts Avenue, Room 1-382, Cambridge, Massachusetts 02139 ATTN: Dr. R. V. Whitman	1

In accordance with letter from DAEN-RDC, DAEN-ASI dated 22 July 1977, Subject: Facsimile Catalog Cards for Laboratory Technical Publications, a facsimile catalog card in Library of Congress MARC format is reproduced below.

Baladi, George Youssef

Response of linear elastic transverse-isotropic media to borehole pressuremeter loadings / by George Y. Baladi and Michael E. George. Vicksburg, Miss. : U. S. Waterways Experiment Station ; Springfield, Va. : available from National Technical Information Service, 1978.

55 p. : ill. ; 27 cm. (Technical report - U. S. Army Engineer Waterways Experiment Station ; S-78-12)

Prepared for Director, Defense Nuclear Agency, Washington, D. C., under DNA Subtask SB209, Work Unit 40, "Material Model Development and Ground Shock Calculations."

References: p. 45.

1. BOREHOLE (Computer program). 2. Boreholes. 3. Boundary value problem. 4. Elastic materials. 5. Isotropic materials. 6. Pressure gages. 7. Pressure measurement. 8. Transverse-isotropic materials. I. George, Michael E., joint author. II. Defense Nuclear Agency. III. Series: United States. Waterways Experiment Station, Vicksburg, Miss. Technical report ; S-78-12.
TA7.W34 no.S-78-12